SSD

SCIENCE FOR A SUSTAINABLE DEVELOPMENT

IMPACT OF BIOGENIC EMISSIONS ON ORGANIC AEROSOLS AND OXIDANTS IN THE TROPOSPHERE

« IBOOT »

J.-F. MULLER, S. COMPERNOLLE, K. CEULEMANS, J. PEETERS, L. VEREECKEN, B. KANAWATI, A. SADEZKY, R. WINTERHALTER, G. MOORTGAT , S. A. CARL, T. LAM NGUYEN, F. HERRMANN, J. VALVERDE-CANOSSA, G. SCHUSTER

ENERGY

TRANSPORT AND MOBILITY

AGRO-FOOD

HEALTH AND ENVIRONMENT

CLIMATE

BIODIVERSITY

ATMOSPHERE AND TERRESTRIAL AND MARINE ECOSYSTEMS

TRANSVERSAL ACTIONS

.be

SCIENCE FOR A SUSTAINABLE DEVELOPMENT
(SSD)

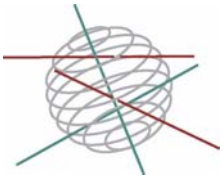

Atmosphere

FINAL REPORT (PHASE I)

IMPACT OF BIOGENIC EMISSIONS ON ORGANIC AEROSOLS AND OXIDANTS IN THE TROPOSPHERE

« IBOOT »

SD/AT/03A

Promotors

Jean-François Muller
Belgian Institute for Space Aeronomy (IASB-BIRA)
Avenue Circulaire 3, B-1180 Bruxelles
Tel.: +32 2 3730366
Fax: +32 2 3748423

Jozef Peeters, Luc Vereecken, Minh Tho Nguyen
Katholieke Universiteit Leuven (KULeuven)

Geert Moortgat, Richard Winterhalter, Jos Lelieveld
Max-Planck Institute for Chemistry (MPI), Mainz, German

Authors

Jean-François Muller, Steven Compernolle, Karl Ceulemans (IASB-BIRA)
Jozef Peeters, Luc Vereecken (KULeuven)
Basem Kanawati, Alexa Sadezky, Richard Winterhalter, Geert Moortgat (MPI)

Co-workers: Shaun A. Carl, Thanh Lam Nguyen (KULeuven), Frank Herrmann, Jessica Valverde-Canossa, Gerhard Schuster (MPI-Mainz)

April 2008

Rue de la Science 8
Wetenschapsstraat 8
B-1000 Brussels
Belgium
Tel: +32 (0)2 238 34 11 – Fax: +32 (0)2 230 59 12
http://www.belspo.be

Contact person:
Mrs Martine Vanderstraeten : +32 (0)2 238 36 10
Project Website: http://www.aeronomie.be/tropo/iboot

J.-F. Muller, S. Compernolle, K. Ceulemans, J. Peeters, L. Vereecken, B. Kanawati, A. Sadezky, R. Winterhalter, G. Moortgat, S. A. Carl, T. Lam Nguyen, F. Herrmann, J. Valverde-Canossa, G. Schuster. ***Impact of biogenic emissions on organic aerosols and oxidants in the troposphere « IBOOT »*** Final Report Phase 1. Brussels : Belgian Science Policy 2009 – 46 p. (Research Programme Science for a Sustainable Development)

Table of Content

ACRONYMS AND ABBREVIATIONS

APCI+	Positive mode of Atmospheric pressure chemical ionization source
APPI	Atmospheric pressure photo ionization
BOREAM	Biogenic compounds Oxidation and Related Aerosol formation Model
BVOC	Biogenic Volatile Organic Compound
CI	Criegee Intermediate
CID	Collision induced dissociation
CID-ESI-	Fragmentation pattern mass spectrum generated from an isolated anion formed from negative mode of Electrospray ionization source
CID-APCI+	Fragmentation pattern mass spectrum generated from an isolated cation formed from the positive mode of APCI ionization source
CTM	Chemistry/Transport Model
DBE	Double bond equivalent
DFT	Density functional theory
E_b	Barrier height (kcal mol^{-1})
ESI-	Negative mode of Electrospray ionization source
FTIR	Fourier Transform infrared
HMPH	Hydroxy methyl hydroperoxide
HPLC	High pressure liquid chromatography
LC-MS-MS-TOF	Liquid chromatography coupled to tandem mass spectrometer with TOF
MCM	Master Chemical Mechanism
MS-MS	Tandem mass spectrometry
NMVOC	Non-methane volatile organic compound
POZ	Primary ozonide
PTR-MS	Proton transfer reaction mass spectrometer
RRKM-ME	Rice-Ramsperger-Kassel-Markus rate theory combined with master equation analyses
SCI	Stabilized Criegee Intermediate
SMPS	Scanning mobility particle sizer
SAR	Structure-Activity Relationship
SOA	Secondary organic aerosol
SOZ	Secondary ozonide
TOF	Time of flight mass spectrometric analyzer
Triple Quad TOF system	a hybrid mass spectrometric analyzer, which consists of three successive linear quadrupoles connected orthogonally to a TOF analyzer through ion pulser with ion mirror (reflectron) to increase the resolution
TST	Transition State Theory
UT	Upper troposphere
X-HP1-C1	A peroxidic oxidation product with nominal mass X generated from hydroperoxide channel 1 of Criegee Intermediate C1
X-NP-HP1-C1	A non-peroxidic oxidation product generated through hydroperoxide channel HP1 of Criegee Intermediate C1
X-HP2-C1	A peroxidic oxidation product with nominal mass X generated from hydroperoxide channel 2 of Criegee Intermediate C1
X-HP-C2	peroxidic oxidation product with nominal mass X generated from hydroperoxide channel of Criegee Intermediate C2
X-E-C2	Oxidation product with nominal mass X generated through the ester channel of Criegee Intermediate C2
ZPVE	Zero point vibrational energy

1. SUMMARY

Human activities and the biosphere release large amounts of reactive gases which have a profound impact on our environment. In contrast with other classes of pollutants, the non-methane volatile organic compounds (NMVOCs) are overwhelmingly biogenic (BVOCs). Secondary pollutants resulting from their oxidation in the air include ozone and aerosols, which are key actors in air quality and climate change issues. Their emissions also influence the oxidizing capacity of the atmosphere, mainly through their impact on the hydroxyl radical (OH). The general lines of their oxidation mechanisms are believed to be well-known, and many processes involved in the formation of Secondary Organic Aerosol (SOA) have been identified. SOA production is generally calculated based on the absorptive theory of *Pankow* (1994) and aerosol yields estimated from smog chamber experiments. However, the use of experimental product yields in atmospheric models is uncertain, due to large differences between the photochemical conditions in experimental setups and in the atmosphere. Near-explicit chemical mechanisms have been elaborated and validated for the degradation of pinenes by OH, up to the formation of primary products (*Peeters et al.,* 2001; *Capouet et al.*, 2004). These studies revealed important differences between the product yields in laboratory conditions and in the atmosphere, due in part to the existence of unexpected reaction sequences. Such detailed mechanisms are still lacking for other important reactions, like the ozonolysis of terpenes, and the degradation of primary products. In particular, the degradation mechanism of the very reactive sesquiterpenes is essentially unknown, in spite of its potentially great importance for new particle formation and SOA growth. Furthermore, heterogeneous and particle-phase reactions are still poorly characterized, although it is now well established that they generate low-volatility oligomers and increase the SOA yields in the oxidation of terpenes.

The IBOOT project adopts an integrated approach consisting of laboratory, theoretical and modeling investigations in order to address these issues and to better quantify the role of biogenic hydrocarbons, in particular with respect to the formation of ozone and aerosols and the oxidation capacity of the atmosphere. More specifically, the chemical degradation and aerosol formation potential of two important sesquiterpenes are investigated in the laboratory at the Max-Planck Institute in Mainz: β-caryophyllene (during Phase 1 of this project) and α-humulene (during Phase 2). The degradation mechanism of monoterpenes (α- and β-pinene) and sesquiterpenes (β-caryophyllene and α-humulene) are constructed by means of advanced theoretical methods in KULeuven, and validated by model simulations of laboratory experiments at IASB-BIRA in Brussels. The aerosols generated from these compounds are characterized by laboratory (Mainz) and modeling (Brussels) studies. The role of specific oxygenated organic compounds in the upper troposphere is also investigated at KULeuven. Finally, a global model will be used (during Phase 2) to test the BVOC oxidation mechanism and aerosol formation potential against field measurements, and to assess the overall importance of BVOC in the atmosphere. The results obtained during the first Phase of this project are summarized below.

Laboratory studies of mono- and sesquiterpene ozonolysis (MPI-Mainz)

Products studies using mass spectrometric methods of the reaction of ozone with the sesquiterpene β-caryophyllene were performed and a reaction mechanism was developed based on the observed products. Moreover, investigations on the applicability of potential analytical methods for the characterization of reactive oxidation products (H_2O_2 and organic peroxides) were conducted. Mechanistic studies included the determination of OH-radical yields from mono- and sesquiterpene ozonolysis and kinetic experiments with the aim to measure the rate constants for ozone with the various double bonds in poly-unsaturated sesquiterpenes. In another study, the aerosol yields from sesquiterpene-ozonolysis were determined under various experimental conditions and finally, in order to improve the understanding of aerosol nucleation processes, the formation of oligomers and polymers from simple alkenes and enol ethers was investigated using several mass spectrometers (LC-MS-MS-TOF, FTICR-MS-MS).

More than 20 components of the secondary organic aerosol (SOA) formed from the ozonolysis of β-caryophyllene were characterized by LC-MS-MS-TOF using two different ionisation methods (ESI^- and $APCI^+$). ESI^- is known as a very sensitive technique for the measurement of carboxylic acids.

Additionally, an ESI^--method was developed to detect not only carboxylic acids anions, but also aldehydes as anions, thus extending the range of detectable products by ESI^-. Measurements with $APCI^+$ (high ionization efficiency of carbonyl groups) completed the investigations and allowed to compare the trace of each anion with its corresponding cation, to yield complementary information about the identity of the product. In depth analysis of CID (Collision Induced Dissociation) spectra of anion-cation pairs led in some cases to unequivocal structural determination. In other cases, where chromatographic co-elution was observed, structural determination of important isomeric oxidation products could be achieved. Besides the detected oxo- and dicarboxylic acids, multi-functional isomeric products bearing e.g. aldehydic, carbonyl and hydroxyl groups could be differentiated by examining their CID fragmentation pathways. Fragmentation mechanisms were proposed for the experimentally observed ions in all the CID experiments. Gas phase deprotonation potentials were calculated by DFT (Density Functional Theory) to estimate the most thermodynamically favourable deprotonation site for efficient negative ion formation in Electrospray (ESI) (*Kanawati et al.,* 2008b).

The OH-radical yields from the ozonolysis of several mono- and sesquiterpenes were indirectly determined using an OH-radical scavenger (cyclohexane), whose reaction product with the OH-radical (cyclohexanone) was quantified by PTR-MS, and from its product yield the OH-radical yield could be calculated. For β-caryophyllene, the OH-radical yield from the second double bond was twice as large (21 %) as for the first more reactive double bond (8.5 %). For α-humulene, the first two double bonds gave the same OH-radical yield of 10 %, the OH yield from the third double bond was not determined (*Herrmann,* 2006).

The experimentally determined rate constant for the ozone attack of the second (less reactive) exocyclic double bond in β-caryophyllene was determined by simulation of the ozone consumption using Facsimile as $k_2 = 1.1 \times 10^{-16}$ cm^3 $molecule^{-1}$ s^{-1}. This value is two orders of magnitude lower than the rate constant for the ozone attack of the first reactive endocyclic double bond in β-caryophyllene, $k_1 = 1.16 \times 10^{-14}$ cm^3 $molecule^{-1}$ s^{-1}. The rate constant for the first, second and third ozone attack in α-humulene is 1.17×10^{-14}, 3.6×10^{-16} and 3.0×10^{-17} cm^3 $molecule^{-1}$ s^{-1}, respectively (*Herrmann,* 2006).

The potential applicability of LC-MS-MS-TOF for the detection of standard peroxides was investigated, with negative results. H_2O_2 and simple α-hydroxy-hydroperoxides could be measured by HPLC. The yields of H_2O_2 were found to be 2 to 4 % for β-caryophyllene, and four times larger for α-humulene. In the aerosol phase also significant quantities of long-chain hydroperoxides (C_6 to C_{12}) were detected, with a relative yield of 12 % compared to H_2O_2.

Although the detected products in these laboratory experiments do not provide unambiguous information on the precise oxidation pathways occurring in the reactor, their nature represent useful constraints in the development of oxidation mechanisms using theoretical means, in particular with regard to the fate of the Criegee Intermediates. This development will be made possible by the ongoing advances in the realization of accurate Structure-Activity-Relationships for important classes of chemical reactions, as well as by the high-level theoretical calculations aiming at determining the fate of key specific intermediates produced in the degradation of the terpenes.

The aerosol yield from β-caryophyllene ranged from 6 to 24 % in the absence of CI-scavenger, while in the presence of CI-scavenger such as HCOOH, HCHO and H_2O the yield ranged from 9 to 41 %. The increasing aerosol yield by addition of water vapour and with higher concentrations of formic acid is unexpected, since previous studies of the ozonolysis with monoterpenes have indicated that the addition of HCOOH decreases the aerosol yields. It is suggested that formic acid adds to the CI to generate an intermediate product with sum formula of $C_{16}H_{26}O_5$, which then undergoes a rearrangement to yield the oxocarboxylic acid β-caryophyllonic acid, a non-volatile compound, and thus increases the aerosol yield. The SOA yield was also found to depend on aerosol mass (*Herrmann,* 2006).

Oligomer formation involving Criegee Intermediates, first observed in the ozonolysis of a variety of enol ethers (*Sadezky et al.,* 2006), was also shown to occur for small symmetric alkenes in an analogous way. The formed SOA was detected by a SMPS system and chemically characterized by a hybrid ESI-MS-MS-TOF technique in the mass range m/z 200–800. The chemical composition was confirmed by accurate mass measurements with an ESI Fourier Transform Ion Cyclotron Resonance (FTICR) mass spectrometer (in cooperation with the University of Giessen), which offers ultrahigh resolution and high sensitivity for the characterization of complex samples. All detected oligomers possess the basic structure of a linear oligoperoxide, $-[CH(R)-O-O]_n-$, with the repeated chain unit CH(R)OO having the same elementary compositions as the main Criegee Intermediates (CI) in these

ozonolysis reactions. The elemental compositions of parent ions, fragment ions and fragmented neutrals determined by accurate mass measurements with the FTICR technique allows to assign a complete structure to the oligomer molecules. It is suggested that the formation of the oligoperoxidic chain units occurs through a new gas-phase reaction mechanism observed for the first time, which involves the addition of stabilized CI to organic peroxy radicals. This oligoperoxide formation involving CI-like chain units represents a new pathway for SOA and oligomer formation and shows its validity for a wide range of alkenes (*Sadezky et al.,* 2008).

Preliminary results for the sesquiterpene α-E,E-farnesene show that also the reactions of ozone with terpenes produce high-molecular weight compounds in the mass range 250 to 800 u. Future work will elucidate the possible formation of oligomers from other sesquiterpenes.

Development of predictive tools for mechanism development (KULeuven)

Progress has been made in the development of Structure-Activity Relationships (SARs) and predictive correlations for some key reaction classes in atmospheric chemistry. Such SARs are highly useful in the construction of atmospheric oxidation mechanisms of larger VOCs, including biogenics. The barrier height E_b for decomposition rate coefficient of alkoxy radicals depends primarily on the α- and β-substituents on either side of the breaking $^{\bullet}OC_{\alpha}–C_{\beta}$ bond. A easily applicable SAR was developed for the prediction of this barrier height, based on a large set of quantum chemical calculations including alkyl-, hydroxy-, oxo-, hydroperoxy-, alkylperoxy-, alkoxy-, nitrate- and nitrite functionalities, as well as unsaturated groups and some ring structures. Recently, a paper was published (*Peeters et al.*, 2007) on the site-specific addition of OH radicals on (poly)unsaturated hydrocarbons, based on the latest kinetic data recommendations available in the literature and direct experimental measurements. This SAR predicts the partial and total rate coefficients as a function of the substitution pattern directly surrounding the double bond or conjugated alkadiene.

A predictive correlation, linking the C–H bond strength to the rate of site-specific H-abstraction from hydrocarbons by OH radicals, is under active development. The data currently includes over 50 radical products and hundreds of conformers. Bond strengths are obtained at various levels of quantum chemical theory, while several models are explored to deduce the site-specific rate coefficients. The results are exported directly to a website, ensuring easy dissemination of the results.

Development of terpene oxidation mechanisms

The OH-initiated degradation of α-pinene was upgraded in a recent publication (*Vereecken et al*., 2007), now including H-shift and ring closure reactions for certain peroxy-radical intermediates. This new chemistry explains the formation of some heavy poly-oxygenated reaction products observed experimentally. The predicted production of hydroperoxides and (hydroxy-)(di-)carbonyl compounds has a profound impact on the predicted SOA formation. The OH-initiated degradation mechanism of β-pinene is under active development, specifically focusing on the dependence of the product distribution on the concentration of NO and HO_2/RO_2. This chemistry is strongly influenced by non-traditional pathways, with (per)oxy radical ring closure reactions affecting most of the chemistry; the predicted product distributions are in good agreement with the scarce experimental data.

The research on the ozone-initiated oxidation of α- and β-pinene currently focuses on the formation of products with (multiple) carboxylic acid functionalities, using a combination of high-level quantum chemical calculations with MC-TST, while explicitly examining reaction through all four Criegee intermediates formed. The O_3-initiated oxidation of β-caryophyllene was investigated theoretically, the prediction being in good agreement with and complementing the extensive experimental investigation detailed in this report. A first-generation product distribution is presented, as well as T-dependent, site-specific and total thermal rate coefficients; this work will be submitted for publication during the first half of 2008. Preliminary work on the ozonolysis of α-humulene revealed that ozone addition on all three >C=C< sites proceeds without barrier, explaining the high total rate, but also implying a highly complex overall mechanism.

Modeling α-pinene degradation

The chemical box model describing the oxidation of α-pinene by OH developed in our previous work (*Capouet et al*., 2004) has been extended to encompass the O_3- and NO_3-initiated oxidation, as well as the new pathways proposed by *Vereecken et al.* (2007). Given the lack of credible pathway leading to the formation of key polyfunctional acids known to be produced in the ozonolysis of α-pinene, an artificial pathway leading to these compounds has been implemented based on laboratory observations. Since a fully explicit terpene oxidation mechanism would be out of reach with the current computing capabilities, the degradation of the primary products is parameterized by the use of an extensive set of generic and semi-generic compounds. This development of our mechanism is based to a large extent on SARs developed within IBOOT by the KULeuven team. The generic compounds are grouped into volatility classes, and can therefore contribute to the growth of SOA.

The complete α-pinene degradation mechanism is published on a web page which allows users to explore it in a convenient way (http://www.aeronomie.be/tropo/boream/). The coupled gas/particle partitioning model, BOREAM (Biogenic compounds Oxidation and RElated Aerosol formation Model) includes about 5000 reactions and 1200 species.

Organic aerosol modeling

Gas/particle partitioning follows the approach of *Pankow* (1994), with vapor pressures calculated following *Capouet and Müller* (2006). In order to account properly for the interactions between the different compounds entering the composition of SOA (including water), a parameterization built on UNIFAC (*Fredenslund et al.*, 1975) has been developed for calculating the activity coefficients. Since the interaction parameters for important functional groups (e.g. nitrates and hydroperoxides) are missing in the published versions of UNIFAC, we have estimated these parameters based on the SPARC calculator (*Hilal et al.*, 2004). The activity coefficient parameterization has been implemented in the organic aerosol model. The impact of non-ideality on SOA formation is found to be small in absence of water uptake, being typically of the order of 10% for individual species, although larger effects are found in the case of low-VOC experiments. When water is allowed to condense on SOA, non-ideality reduces the aerosol yields, especially at high relative humidity, due to repulsion between water and organics.

The α-pinene degradation mechanism and SOA formation model has been tested against a large number of laboratory experiments: about 30 photooxidation experiments and over 100 dark ozonolysis experiments from a total of 15 published studies. The model generally reproduces the measured SOA yields to within a factor of 2, a remarkable result considering the uncertainties on the vapour pressures and the preliminary nature of the ozonolysis mechanism. This relatively good agreement contrasts with the large underestimations of SOA found in several previous modelling studies, which found necessary to increase the partitioning coefficients by orders of magnitude in order to match the laboratory data. As expected, the formation channels leading to pinic acid and hydroxy pinonic acid have a strong influence on the yields, stressing the need for further efforts aiming at their elucidation.

Two types of oligomerization reactions have been tested with the model. The particle-phase association reactions of aldehydes and hydroperoxides are found to have only a moderate impact on the SOA yields, except in a few cases where the calculated yields were already high in absence of such reactions. The gas-phase oligomerization of stabilized Criegee Intermediates is found to be significant in the low-VOC ozonolysis experiments.

The temperature dependence of the SOA yields is not correctly reproduced by the model. The calculated SOA yields decrease rapidly when temperature increases, as a result of the temperature dependence of vapour pressures. The experiments indicate that SOA is formed in significant amounts even at high temperatures, suggesting the existence of unknown channels leading to extremely condensable compounds.

Impact of oxygenates on the upper troposphere

The reactions of oxygenates with OH are characterized by the formation of H-bonded pre-reactive complexes (PRC), affecting the energy of the abstraction transition states (TS), and resulting in

complex temperature- and pressure dependences. Several papers are in preparation, detailing the different regimes of reaction, and illustrating some of the effects for complex reactants, including (deuterated) carboxylic acids.

The reactions of HO_2 radicals with some major carbonyl-bearing products of the isoprene and terpene degradation were investigated. The results indicate that these reactions, combined with subsequent reactions with NO/HO_2, can constitute effective sinks for some of these compounds near the tropopause. Additionally, we theoretically investigated the reactions with HO_2 of α-hydroxy-alkylperoxy adducts, formed in the HO_2 + carbonyl reactions as well as from α-hydroxy alkyl radicals. Recent experimental evidence indicates that these reactions have higher yields of alkoxy- and OH radicals than previously assumed. Papers are in preparation.

2. INTRODUCTION

2.1 Context

The biosphere emits large amounts of reactive gases having a profound environmental impact. Pollutants generated from their oxidation include ozone and aerosols, which are key players in air quality and climate change. They influence also the oxidizing capacity of the atmosphere, through their impact on the hydroxyl radical. The non-methane volatile organic compounds (NMVOCs) are primarily biogenic (BVOCs). Although the general lines of their oxidation mechanisms are believed to be well-known, and processes involved in the formation of Secondary Organic Aerosols (SOA) have been identified, recent findings suggest that the current models and mechanisms are incomplete. In particular, it is now recognized that detailed BVOC degradation mechanisms validated by carefully designed laboratory experiments are required in order to reliably extrapolate the impact of BVOCs in the atmosphere. Such mechanisms are still lacking for important BVOC classes, like the monoterpenes ($C_{10}H_{16}$) and sesquiterpenes ($C_{15}H_{24}$). Furthermore, the current gas/aerosol partitioning models appear to be unable to match the aerosol yields from laboratory experiments, possibly because of unaccounted processes such as polymer and oligomer formation. In spite of their probable high relevance in the troposphere, their impact is still unknown. Finally, the loss mechanisms of important oxygenated compounds are still very uncertain upper tropospheric conditions. For example, the reactions of carbonyl compounds with HO_2 are potentially significant in this region, a finding of importance for the budget of radicals and ozone.

2.2 Objectives and expected outcomes

We propose to conduct laboratory, theoretical and modelling investigations aiming at reducing the large uncertainties associated with the impact of biogenic volatile organic compounds emissions in the atmosphere. Our general objective is to establish the photochemical degradation mechanism and aerosol formation potential of several mono- and sesquiterpenes. Our specific objectives are the following:

1) Experimental determination of the composition and yields of the organic aerosol formed in the ozonolysis of the sesquiterpenes β-caryophyllene and α-humulene in atmospheric conditions (MPI). The influence of (i) H_2O and other Criegee-Intermediate scavengers (HCOOH and HCHO), (ii) different OH-radical scavengers, (iii) temperature (between 275 and 305 K) will be investigated in order to clarify the reaction mechanism. Polymer/oligomer formation and the CCN activity of aerosols from mono- and sesquiterpene + ozone reaction will be determined.

2) Development of predictive tools for mechanism building, based on advanced theoretical calculations (KULeuven). These tools are needed to estimate the reaction parameters in a given reaction class from the available data for individual compounds.

3) Gas-phase mechanism development for (i) the oxidation of α- and β-pinene by OH, and (ii) the ozonolysis of α-pinene, β-caryophyllene and α-humulene (all partners). The formation of key low-volatility compounds should be elucidated. Reduced mechanisms will be derived for implementation in atmospheric models. These mechanisms will be validated against laboratory results obtained under various conditions.

4) Gas/particle partitioning model development (IASB-BIRA), including the determination of the vapour pressures, activity coefficients and solubilities of the products. The role of aqueous phase chemistry and inorganic salts will be represented, since they might favour heterogeneous reactions enhancing the aerosol yields. The partitioning module coupled to the gas-phase oxidation model will be evaluated against laboratory results.

5) Study of the reactions of oxygenated compounds (e.g. acetic acid, hydroxyacetone, glycolaldehyde, glyoxal, nopinone) with OH and/or HO_2 in the conditions of the upper troposphere (KULeuven).

6) Assessment of the global impact of terpenes on the budget of oxidants and aerosols, using a global CTM (IASB-BIRA). The modelled organic aerosol will be validated against field measurements.

7) Valorization and dissemination (all), including (i) a website for Structure-Activity Relationships (ii) a workshop on mechanism development, in collaboration with BIOSOL, and (iii) data submission to international databases.

3. PROGRESS AND IMPLEMENTATION OF THE METHODOLOGY

3.1 Laboratory studies of mono-and sesquiterpenes ozonolysis (Mainz)

3.1.1 *Products and reaction mechanism of the reaction of ozone with the sesquiterpene β-caryophyllene*

The reaction of ozone with the sesquiterpene β-caryophyllene has been studied in a 570 L glass reactor at atmospheric conditions. For the analysis of gas-phase products (e.g. CO, CO_2, HCOOH and HCHO) on-line FTIR spectroscopy was applied. Particulate products were sampled on teflon (PTFE) filters and extracted with methanol and analyzed by liquid chromatography-mass spectrometry (LC/MS) using Electrospray ionization (ESI-) and Atmospheric Pressure Chemical Ionization (APCI+). Due to differences in ionization efficiencies of organic compounds with different functional groups, the combination of ESI- and APCI+ mass spectra gives complementary information for the identification of functional groups. Furthermore, collisional induced dissociation (CID) experiments of parent ions were performed to gain structural information. DFT (Density Functional Theory) calculations were performed to calculate site dependent proton affinities and deprotonation potentials of the structural isomers.

The reaction of Criegee-Intermediates (CI), which are formed by decomposition of the primary ozonide, with H_2O is a NO_x-independent source of hydroperoxides and was investigated at various relative humidities. The formation of H_2O_2 and organic hydroperoxides during ozonolysis of β-caryophyllene and α-humulene was monitored by HPLC with fluorescence detection. Furthermore, experiments with other Criegee-Intermediate scavengers like HCOOH and HCHO were also performed in order to elucidate the reaction mechanism. Proton transfer reaction mass spectrometry (PTR-MS) was used to determine the OH radical yields by use of a scavenger method.

Mass spectrometric characterization and identification of oxidation products from β-caryophyllene

β-Caryophyllene contains two double bonds with different reactivities toward O_3. The rate constant of the endocyclic double bond (1) is nearly 100 times larger than the exocyclic double bond (2) (see kinetics section 3.1.3).

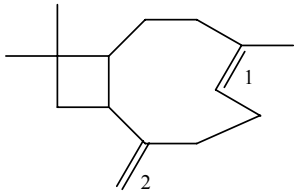

The analysis of particulate-phase products in the aerosol samples by LC/MS using two different ionization sources (ESI- and ACPI+) has provided useful insights on the identification of the products of the β-caryophyllene ozonolysis. The identified oxidation products from aerosol samples with reactant ratio β-caryophyllene to ozone of 1.5 to 1 are shown in Figure 1.

From the β-caryophyllene (m=204 g/mole) structure and the general ozonolysis mechanism it is possible to predict different products (*Winterhalter et al.*, 2000; *Koch et al*., 2000; *Jaoui et al.*, 2003*)*, as depicted in Figure 2. The framed oxidation products are identified in this work, whereas the product in shaded framed were also shown by *Jaoui et al*. (2003). The roman numbers indicate the products shown in Figure 1.

The internal double bond (1) reacts first with O_3, producing 2 Criegee intermediates **CI-1** and **CI-2**. Both compounds are the products of the decomposition of the primary ozonide (**POZ**), which is formed when ozone attacks the endocyclic double bond. Possible rearrangements of the Criegee-Intermediates from β-caryophyllene ozonolysis are either the **ester channel** or the **hydroperoxide channel** to generate various oxidation products. Both Criegee intermediates can also be pressure-stabilized forming **Stabilized Criegee-Intermediates SCI**, which may further react with H_2O,

forming β-caryophyllone aldehyde (XI) and H_2O_2, or with HCOOH producing a hydroperoxyformiate. The SCI can also undergo ring closure to form a secondary ozonide (**SOZ**) (*Donahue et al.*, 2005). These products of the SCI reactions are also shown in Figure 2.

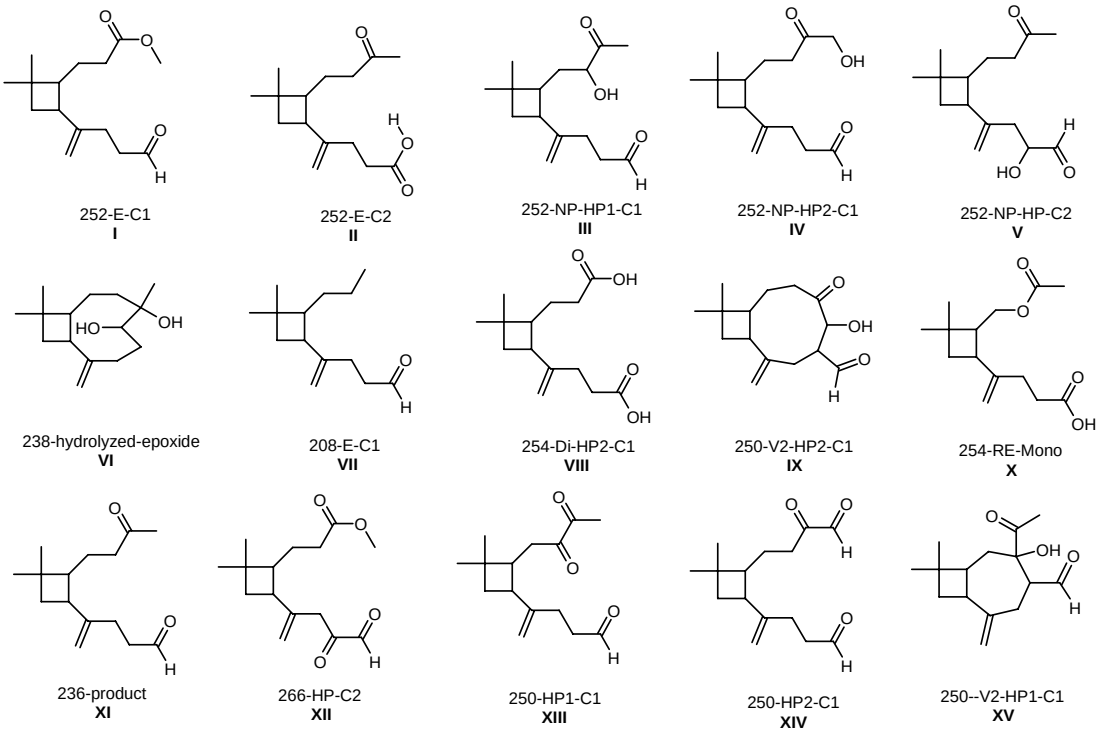

Figure 1. Oxidation products from β-caryophyllene ozonolysis with excess β-caryophyllene.

Assignment of the products of the Ester and Hydroperoxide channels

A large number of multifunctional oxidation products (see Figure 1) could be detected from the aerosol samples, and structures have been deduced using collision induced fragmentation of molecular ions. Moreover, the identification of several isomers with e.g. molecular weight 252 was accomplished with this method and confirmed by theoretical investigations of the fragmentation pathways. An Electrospray method was developed to ionize not only organic acids but also aldehydes in the negative mode, extending widely the range of oxidation products that can be detected in one analysis step (*Kanawati et al.,* 2008b).

Several rearrangements and degradation products of the Criegee-Intermediates CI-1 and CI-2 (with mass 252) are formed through the ester channels and through the hydroperoxide pathways (see Figure 2). In order to facilitate the description of the different products, the molecular weight of the species is indicated in Figure 1, as well as the origin of each Criegee Intermediate. Isomers with NP-HP codes indicate non-peroxidic structures which are believed to be generated from Criegee-Intermediates through hydroperoxidic (HP) channels. The isomers coded with letter E are believed to be formed from ester (E) channels.

Figure 2 shows the structure of the 3 resolved isomers with a neutral nominal mass of 252 formed via the hydroperoxide channel. After OH elimination and reaction with O_2, a series of hydroxyketone-(III, IV, V) and diketone-(XIII and XIV) type products are generated. The diacid β-caryophyllinic acid (VIII) is also generated after several rearrangement steps via the hydroperoxide channel. Two isomers with mass 252 are believed to be formed from the ester channel via a dioxiran intermediate. The products I and II (β-caryophyllonic acid) have been identified unequivocally and attributed to the ester channel.

A detailed study of the ozonolysis of β-caryophyllene was performed by *Jaoui et al*. (2003), who identified 16 gas and particulate reaction products using a combination of HPLC liquid chromatography and GC-MS (operated in the electron impact or chemical ionization mode). They reported a wide range of ring retaining and ring opening products in the gas and particulate phase over

the course of the reaction. However, contrary to our work, their experiments were conducted with excess ozone over β-caryophyllene, which caused both the endocyclic and exocyclic double bonds to be attacked. Only five common products could be assigned.

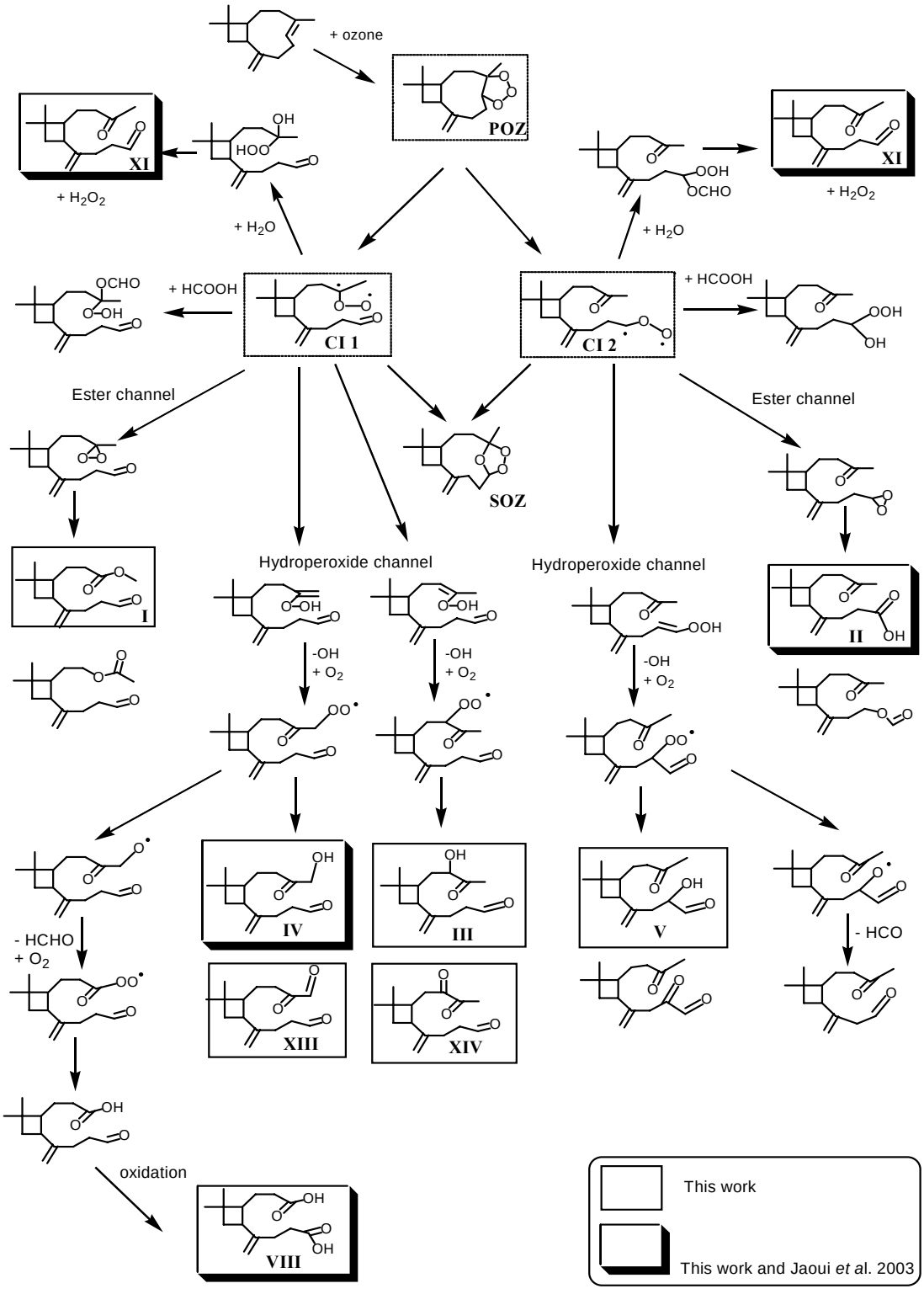

Figure 2: Mechanism of the ozonolysis of β-caryophyllene. Framed oxidation products are identified in this work, whereas the product in shaded framed were also shown by Jaoui et al. *(2003)*. The roman numbers indicate the products shown in Figure 1.

An example is the detection of β-**caryophyllinic acid,** a dicarboxylic acid with structure **VIII** (254-Di-HP2-C1) and molecular mass 254. Figure 3 shows the time dependent trace of anions with m/z=253. The fragmentation pattern of one parent anion $[M-H]^-$ that is generated from this neutral species is also shown in Figure 4 and reveals the existence of two distinct fragmentation pathways

Eq. 1.1 $253^- – (- H_2O) \rightarrow 235^- – (- CO_2) \rightarrow 191^-$

Eq. 1.2 $253^- – (- CO_2) \rightarrow 209^- – (- H_2O) \rightarrow 191^-$

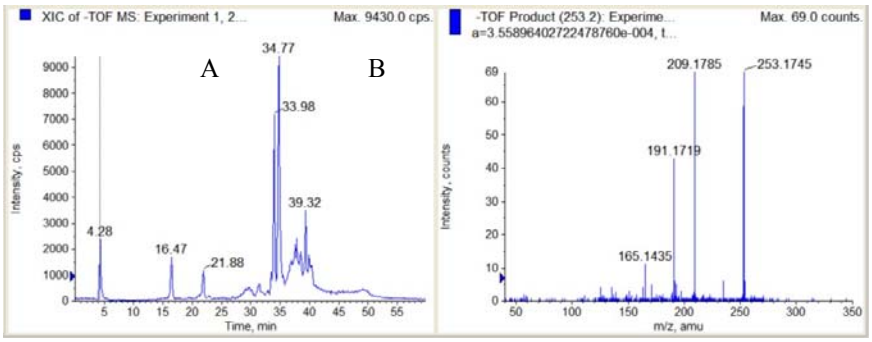

Figure 3. A: Extracted ion chromatogram of m/z 253. B: CID spectrum of the peak at retention time 4.28 min.

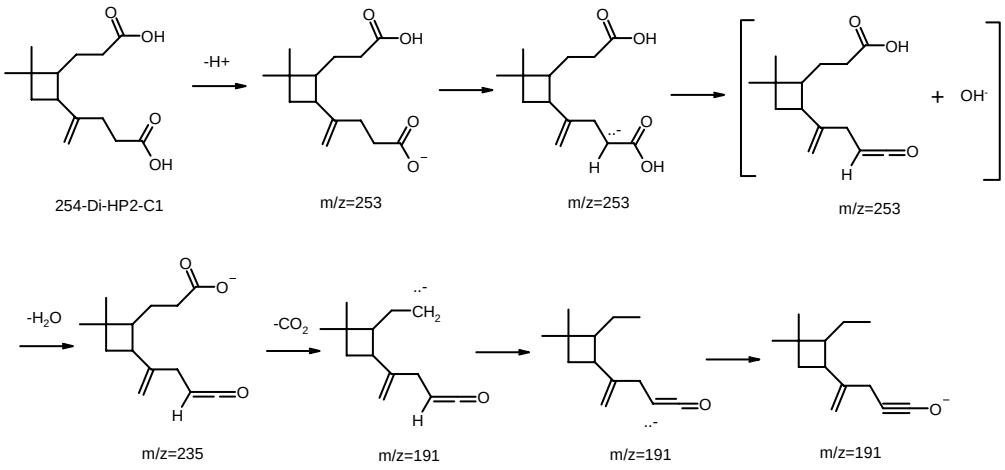

Figure 4. Fragmentation mechanism in agreement with the observed pathway shown in Eq.1.1.

As seen in Figure 4, the neutral dicarboxylic acid 254-Di-HP2-C1 **(VIII)** is deprotonated to yield a carboxylate anion, which can undergo a 1,2-H-shift to form an isomer, in which the negative charge resides in the α-C position relative to the carboxyl group. This ion can be stabilized by ketenization to release an OH^- ion and the latter can form an ion-neutral complex with the ketene neutral. One proton abstraction from the other carboxyl group (in the upper C_4-carbon chain) by the OH^- within this complex eliminates water and forms another carboxylate anion. The new anion (primary fragment ion) can then release CO_2 and the negative charge can move to the lower carbon chain to form a stable deprotonated ketene (secondary fragment ion).

This ion is very stable due to electron delocalization. *Kanawati et al.* (2007, 2008a) have performed extensive CID and DFT studies to elucidate the unusual gas phase ion fragmentation mechanisms of some small oxocarboxylic acids. Both studies confirm water elimination from mono and oxocarboxylic acids (*Römpp et al.,* 2006) The second fragmentation pathway can be also observed from the same parent anion, so that a competition between the two pathways (Eq. 1.1 and 1.2) occurs

and both fragmentation pathways can be observed experimentally, if excess internal energy is available.

Proposed mechanisms for all observed CID fragmentation pathways of parent anions that correspond to the identified oxidation products in the organic aerosol were investigated and discussed in detail by *Kanawati et al*. (2008b). Structures of the most prominent identified products were optimized by the use of quantum mechanical (Density Functional Theory) DFT calculations on the B3LYP/6-311+G(2d,p)//B3LYP+G(d)+ ZPVE theoretical level and the site dependent deprotonation potentials from different acidic positions in each product were calculated (*Kanawati et al.*, 2007, 2008a), to determine the identity of the most probable parent anion for further CID studies.

Summary of the reaction mechanism of the ozonolysis of β-caryophyllene

A condensed mechanism of the reaction of O_3 with β-caryophyllene is displayed in Figure 5. Here the fate of the different reaction channels of the Criegee Intermediates is summarized based on the results obtained in this study. The contribution of the hydroperoxide channel was estimated to 10%, uniquely based on the yield of the OH radicals for the first double bond (see section 3.1.2). OH radicals are formed by the decomposition of the hydroperoxides intermediates after H-shift within the CI (*Johnson and Marston,* 2008) (see also Figure 2). The amount of stabilisation was estimated from experiments performed in the presence of HCOOH. During the ozonolysis of β-caryophyllene, the HCOOH concentration decreased by 60 %, as is seen in Figure 6. This decay was attributed to the effective scavenging reaction of HCOOH with the SCI. The total contribution of the stabilisation was estimated as > 80 % because the SCI can also undergo ring closure to produce SOZ (see Figure 2), which has been predicted by theoretical calculations to be important for endocyclic compounds with 15 carbon atoms (*Donahue et al.*, 2005). An estimation of the contribution to ester channel could be made based on the yield of the main products (I) and (II). These compounds were qualitatively detected but not quantitatively assessed. A yield of 5-10% can be inferred from the sum of the yields of all channels.

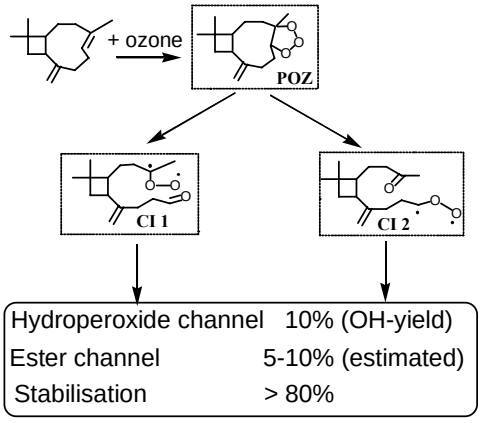

Figure 5. Summary of the reaction channels of the Criegee Intermediates CI-1 and CI-2 from the β-caryophyllene ozonolysis.

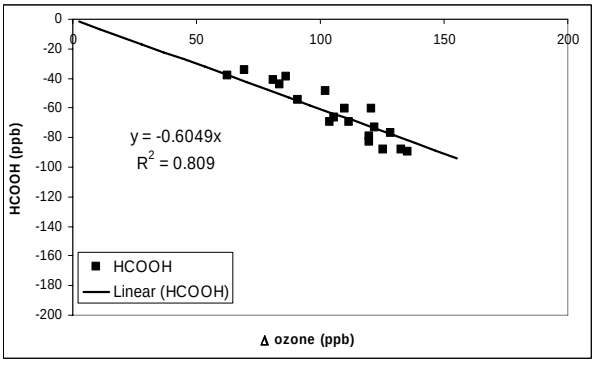

Figure 6. Decrease of HCOOH due to reaction with the SCI from β-caryophyllene.

3.1.2 *OH-radical yields from mono- and sesquiterpene ozonolysis*

For the determination of the yield of the OH radicals, cyclohexane was added as an OH radical scavenger during mono- and sesquiterpene ozonolysis experiments. The selected concentration of cyclohexane insures that about 80% of the OH-radicals were scavenged. The known reaction products are cyclohexanol (yield 35%) and cyclohexanone (yield 53%) (*Berndt et al*., 2003). The concentration of cyclohexanone was followed on-line by Proton Transfer Reaction Mass Spectrometry (PTR-MS) (*Lindinger et al*., 1998). Cyclohexanol looses H_2O to yield m/z=83, which is also formed from cyclohexane + O_2^+ in the ion source, and is therefore not suited as a tracer for OH. For terpenes with more double bonds, the yield of cyclohexanone reflects the OH yield arising from the reaction of O_3 with all double bonds within each terpene. Since in most cases k_1 for the first DB is known, it is possible to differentiate between the OH from the first and other double bonds. This is indicated in Table 1 as 1.DB OH-yield and 2.DB OH-yield. The last column reports yields from other studies. For α-pinene, our value (93%) is somewhat larger but consistent with the literature data (68-91%). Also for β-caryophyllene the measured 1.DB OH-yield of 7.5 and 9% (measured in two experiments) is comparable to the literature value of 6.6% (*Shu and Atkinson,* 1994). α-Humulene has three double bonds, but the rate constant for the third DB is too slow (see below) to measure the OH-yield of the third DB. The sum of the yields of the 1. and 2. DB agree with the cited literature value, which was obtained with excess ozone. For the other terpenes, however, the measured 1.DB OH yield is definitely lower than in previous studies.

Table 1. OH-Radical-Yield in the ozonolysis of mono- and sesquiterpenes.

Alkene	Terpene / ppb	1.DB OH-Yield %	2.DB OH-Yield %	Literature yield 1. DB %
β-Caryophyllene	97.8	7.5	19.9	6 [1)]
β-Caryophyllene	77.0	9.5	22.1	6 [1)]
α-Humulene	64.0	11.4	11.4	22 [1)]
α-Humulene	80.9	9.0	9.0	22 [1)]
α-Phellandrene	104.5	18.6	32.6	
α-Pinene	111.0	93.0	-	85 [2)]; 76 [3)]; 70 [4)]; 83 [5)]; 91 [6)]; 77 [7)]; 68 [8)]
α-Terpinene	116.3	16.7	-	38 [7)]
α-Terpinene	235.9	12.4	-	38 [7)]
γ-Terpinene	99.5	51.3	-	81 [7)]
Myrcene	104.5	30.2	-	115 [2)]; 63 [7)]
Ocimene	102.8	28.4	40.2	63 [2)]; 55 [7)]
Terpinolene	104.5	44.2	-	103 [2)]; 74 [7)]

[1)] Shu et Atkinson (1994); [2)] Atkinson et al. (1992); [3)] Chew and Atkinson (1996); [4)] Paulson et al. (1997); [5)] Rickard et al. (1999); [6)] Siese et al. (2001); [7)] Aschmann et al. (2002); [8)] Berndt et al. (2003).

3.1.3 *Kinetic experiments: rate constants for ozone with the various double bonds*

The experimentally determined rate constant for the ozone attack of the second (less reactive) exocyclic C=C bond in β-caryophyllene was determined by simulation of the ozone consumption using Facsimile as $k_2 = 1.1 \times 10^{-16}$ cm^3 molecule^{-1} s^{-1}. This value is two orders of magnitude lower than the rate constant for the ozone attack of the first reactive endocyclic C=C bond in β-caryophyllene, $k_1 = 1.16 \times 10^{-14}$ cm^3 molecule^{-1} s^{-1}. The rate constant for the first, second and third ozone attack in α-humulene is 1.17×10^{-14}, 3.6×10^{-16} and 3.0×10^{-17} cm^3 molecule^{-1} s^{-1}, respectively (*Herrmann,* 2006). The Facsimile simulation

of the ozone concentrations during the ozonolysis of β-caryophyllene and α-humulene are shown in Figure 7.

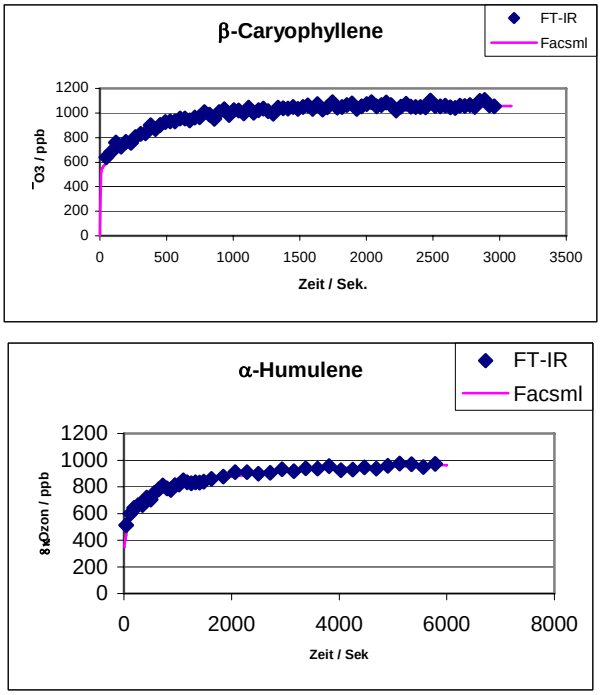

Figure 7. Consumption of ozone versus reaction time for β-caryophyllene and α-humulene. The reaction rates were obtained by simulation using Facsimile.

3.1.4 *Determination of aerosol yields from sesquiterpene-ozonolysis*

The ozonolysis experiments for the determination of SOA mass yields were performed in the absence of OH scavenger. The experiments were performed under 1.5 to 3 fold terpene excess over O_3. The typical time evolution of particle size distributions during the first 60 minutes of the ozonolysis of β-caryophyllene is shown in Figure 8a. The aerosol number reaches its maximum within the first 10 minutes, with a particle diameter of about 50 nm. At longer reaction times particles grow in size, reaching a diameter of 120 nm after 60 minutes reaction time. Their number gradually decreases due to coagulation of the aerosol particle, condensation of semi-volatile compounds on exiting particles, and/or loss by deposition on the reactor wall. The corresponding aerosol mass is shown in Figure 8b.

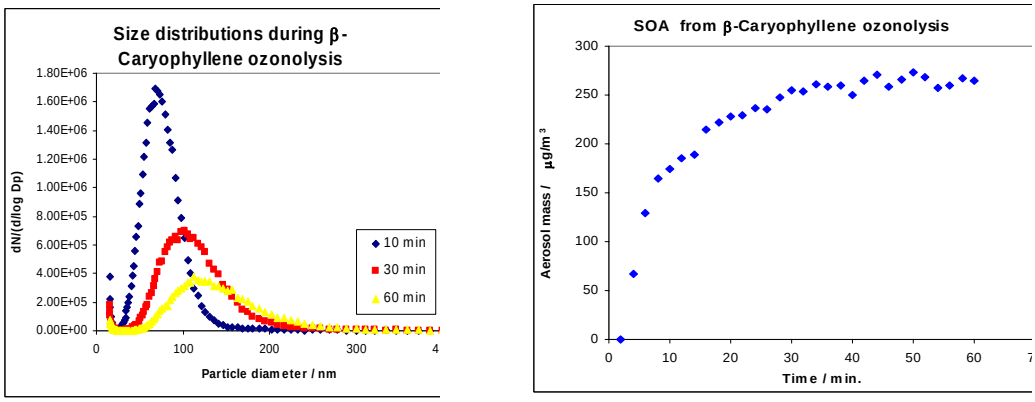

Figure 8. a) Particle size distribution during the first 60 minutes during the ozonolysis of β-caryophyllene; b) Corresponding aerosol mass during the ozonolysis of β-caryophyllene.

From the formed aerosol mass and the reacted β-caryophyllene SOA mass yields have been calculated. Table 2 lists the aerosol yields of β-caryophyllene ozonolysis from different experiments. Some of the experiments were performed in the presence of formic acid, formaldehyde and water as Criegee-Intermediate scavenger. As can be noticed from Table 2, the aerosol yield increases by addition of water vapour and with higher concentrations of formic acid. This increase in aerosol yield is unexpected, since previous studies of the ozonolysis with monoterpenes have indicated that HCOOH acts as an effective Criegee intermediate scavenger (*Bonn et al.*, 2002). It is suggested that formic acid adds to the Criegee Intermediates CI-1and CI-2 (see Figure 2) to generate a formiate product (MW=298) with sum formula of $C_{16}H_{26}O_5$**,** which can then undergo a rearrangement to yield the oxocarboxylic acid β-caryophyllonic acid (**II**) (see Figure 2) and thus increases the aerosol yield.

A temperature-controlled flow tube was set-up to investigate the temperature dependence of the SOA yield for the ozonolysis of β-pinene. It was found that under dry conditions the SOA yield increased for low particle mass concentration (10 μg m^{-3}) from 0.08 at 303 K to about 0.20 at 263 K (*Stenby et al.*, 2007).

Table 2. Aerosol yields from β-caryophyllene (BC) ozonolysis with and without CI-scavenger.

Ozone ppb	BC ppb	Reacted BC μg m^{-3}	Aerosol μg m^{-3}	Aerosol yield %	Scavenger ppb
100	309	920	50	6	-
180	562	2340	190	8	-
200	301	1930	170	9	-
200	315	2310	230	10	-
180	566	2010	210	10	-
200	300	2290	280	12	-
200	320	1540	270	18	-
100	258	1540	370	24	-
200	305	1580	310	19	HCOOH / 250
200	298	2190	460	21	HCOOH / 250
200	298	1900	470	24	HCOOH / 500
200	304	2220	660	30	HCOOH / 500
200	320	1900	620	32	HCOOH / 1000
200	301	2190	820	38	HCOOH / 1000
200	331	1520	620	41	HCOOH / 1000
200	315	2130	180	9	HCHO / 7800
100	239	1050	130	12	HCHO 6800
200	295	1620	440	27	H_2O 12800 ppm *
200	296	1510	420	28	H_2O 12800 ppm *

* This corresponds to 36 % relative humidity

3.1.5 *Identification and quantification of H_2O_2 and organic peroxides*

1. Iodometry of samples collected in the in the gas and aerosol phase gave qualitative indications of the presence of H_2O_2 and organic peroxides.

2. The potential applicability of LC-MS-MS-TOF for individual peroxide detection was investigated, especially with regard to sample treatment of the unstable peroxides, chromatographic separation and ionization method (i.e. ESI and APCI). Samples of the following peroxides: *tert*-butyl hydroperoxide, di-*tert*-butyl peroxide, cumene hydroperoxide and peracetic acid were injected directly to the mass spectrometer through Electrospray. In negative mode, only *tert*-butyl hydroperoxide could be ionized. The investigations have shown that both methods were not suitable for peroxide detection.

3. The applicability of the existing HPLC method for detection of H_2O_2 and simple α-hydroxy-hydroperoxides was tested for the detection of higher hydroperoxides from mono- and sesquiterpene-ozonolysis. Experiments have been performed in the above described glass reactor at 730 Torr and room temperature. In total, 11 experiments were carried out under the following experimental conditions: relative humidity was between 50 to 60 %, and initial reactant mixing ratios were about 400 ppb of the sesquiterpene and 270 ppb, 860 ppb and 1200 ppb of ozone. Excess cyclohexane (300 ppm) was added as an OH scavenger in some experiments. Preliminary results show that for β-caryophyllene, yields of H_2O_2 were found to be 2 % with excess alkene and 4 % with excess ozone. Moreover, 0.2 % of hydroxymethyl hydroperoxide (HMHP) were formed with excess ozone, while its concentrations were below the quantification limit with excess alkene. Under similar initial conditions, α-humulene produced four times more H_2O_2. The addition of excess cyclohexane as an OH scavenger did not have any detectable influence on H_2O_2 yields for both sesquiterpenes. Extracted filter samples of organic aerosol showed significant quantities of hydroperoxides, with a relative percentage of long-chain (C_6 to C_{12}) organic hydroperoxides to H_2O_2 of up to 12 %.

3.1.6. *Formation of oligomers and polymers from alkene ozonolysis*

An important fraction of secondary organic aerosol (SOA) formed by atmospheric oxidation of diverse volatile organic compounds (VOC) has recently been shown to consist of high-molecular weight oligomeric species. The reactions of ozone with a series of terpenes have produced high-molecular weight compounds in mass range 250 to 800 u, as is shown for the sesquiterpene α-E,E-farnesene in Figure 9 (*Bernard et al., 2008*).

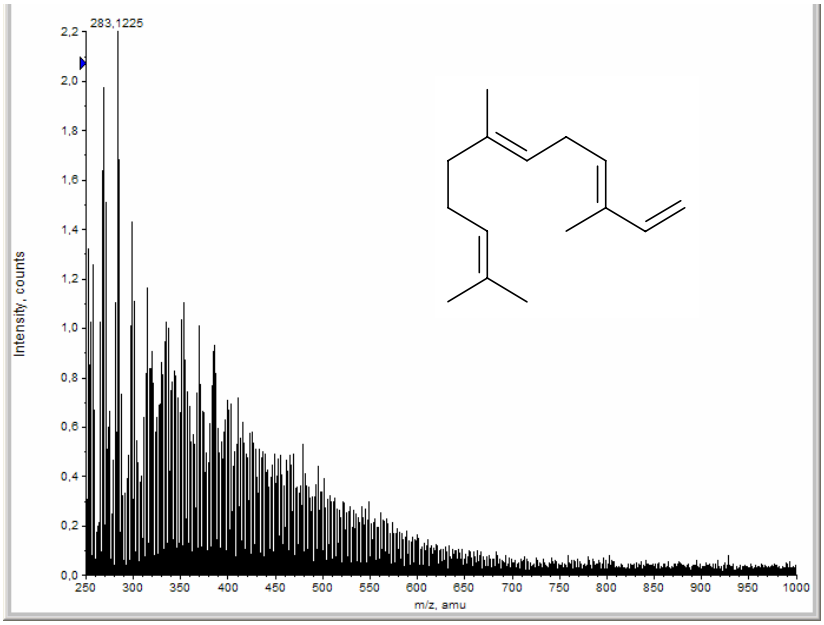

Figure 9. ESI(-)/MS-TOF spectra resulting from the analysis of SOA generated from the ozonolysis of the sesquiterpene α-E,E-farnesene.

In our recent studies we reported the discovery of oligomeric compounds by chemical analysis of secondary organic aerosol (SOA) formed during ozonolysis of enol ethers and structurally related small alkenes (*Sadezky et al.*, 2006; 2008). The formed SOA has been detected by a SMPS system and chemically characterized by a hybrid ESI/MS/MS-TOF technique in the mass range m/z 200–800. The chemical composition was confirmed by accurate mass measurements with an ESI Fourier Transform Ion cyclotron resonance (FTICR) mass spectrometer, which offers ultrahigh resolution and high sensitivity for the characterization of complex samples.

All detected oligomers have the basic structure of a linear oligoperoxide, -[CH(R)-O-O]$_n$-, with the repeated chain unit CH(R)OO having the same elementary compositions as the main Criegee Intermediates (CI) in these ozonolysis reactions. The elemental compositions of parent ions, fragment ions and fragmented neutrals determined by accurate mass measurements with the FTICR technique allow us to assign a complete structure to the oligomer molecules, as exemplary shown in Figure 10.

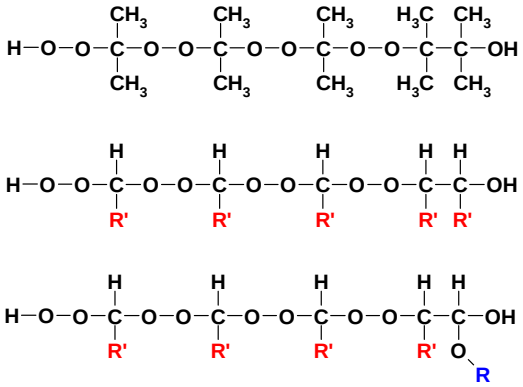

Figure 10. Oligoperoxidic structures suggested for the oligomers formed during gas-phase ozonolysis of enol ethers and symmetric alkenes: *top*: 2.3 dimethyl-2-butene; *middle*: *trans*-3-hexene with R' = C_2H_5 or *trans*-4-octene with R' = C_3H_7; *bottom*: enol ether e.g. ethyl butenyl ether with R = R' = C_2H_5.

We suggest that the formation of the oligoperoxidic chain units occurs through a new gas-phase reaction mechanism observed for the first time in our present work, which involves the addition of stabilized CI to organic peroxy radicals (*Sadezky et al.*, 2008). This oligoperoxide formation involving CI-like chain units represents a new pathway for secondary organic aerosol and oligomer formation and shows its validity for a wide range of alkenes.

3.2 Development of predictive tools for mechanism development (KULeuven)

3.2.1 *SARs for unimolecular alkoxy radical reactions*

The decomposition rate coefficient of alkoxy radicals formed as intermediates in the atmospheric degradation of most hydrocarbons can be well described as $k(T)=A\times\exp(-E_b/kT)$, with the TST frequency factor $A \approx 1.8\times10^{13}$ s^{-1} for nearly all alkoxy radicals, and where the barrier height E_b to decomposition depends strongly on the α- and β-substituents on either side of the breaking $^{\bullet}OC_\alpha–C_\beta$ bond.

$$>C_\alpha O^{\bullet}–C_\beta< \quad \rightarrow \quad >C_\alpha=O \; + \; ^{\bullet}C_\beta<$$

The quantum chemical methodologies applied to this reaction class includes the DFT functionals B3LYP, MPW1K, MPWKCIS1K, and BB1K, and the MP2 *ab initio* methodology combined with DIDZ, 6-31G(d,p), 6-311++G(2df,2pd), and aug-cc-VTZ basis sets, in combinations limited by our computational resources and selected based on the relative merit of the methodologies. Based on results for over 80 transition states with different combinations of 10 substituents, and pending the finalization of the statistical analysis of our current results and cross-validation against higher-order correlated methods, the impact of α- and β-substituents X on the barrier height for alkoxy radical decomposition can be summarized as follows:

$$E_b \,/\, \text{kcal mol}^{-1} = 17.5 + \sum a_x \cdot n_x \cdot X$$

where n_x is the number of substituents of type X on carbon α or β, a_x is the impact of a substituent of type X on the barrier height, and summed over all substituents on carbons α and β. The substituent activities, in kcal mol^{-1}, are listed in the table below:

Table 3: Alkoxy decomposition SAR activities

α-alkyl :	-2.1	β-alkyl :	-3.2

α-OH :	-8.0	β-OH :	-8.0
α=O :	-12.0	β=O :	-8.0
α-OR (R=alkyl) :	-8.9	β-OR (R=alkyl) :	-8.9
α-OOH:	-8.2	β-OOH:	-9.2
α-OOR (R=alkyl) :	-6.3	β-OOR (R=alkyl):	-7.5
α-ONO_2 :	-3.1	β-ONO_2 :	-2.7
α-ONO :	-4.1	β-ONO :	-6.2
α =C< :	+21.1	β =C< :	+4.6
α-C=C< :	-5.0	β-C=C< :	-9.6

In addition, the effect of ring strain has been examined for small rings, where either C_α or C_β is part of a (different) ring system. Three-membered rings with an oxy radical functionality are not stable and spontaneously break the ring. For systems where one of C_α and/or C_β are in a different ring system, the activities are listed in Table 4 for 3- and 4-membered rings. These activities include the effect of the alkyl chain constituting the ring proper. Systems where C_α and C_β are part of the same ring have not been examined yet.

Table 4: Alkoxy decomposition SAR ring activities

C_α in 3-membered ring : *N/A*	C_β in 3-membered ring : +2.4
C_α in 4-membered ring : -2.1	C_β in 4-membered ring : -4.2

Compared to earlier work (*Peeters et al*., 2004) which examined the effect of alkyl-, hydroxy (-OH), and oxo (=O) substituents on the barrier height, the range of substituents was significantly extended to include more oxygen-bearing functionalities, including these in ethers, hydroperoxides, alkylperoxides, nitrates, and nitrites. This will enable us to predict the reactivity for a much wider range of (oxygenated) intermediates formed in the degradation of the larger biogenic hydrocarbons including terpenes and sesquiterpenes. Also, the effect of vinyl and allyl-substituents was investigated to support work on the degradation mechanism of poly-unsaturated hydrocarbons (including ringed structures) such as isoprene and the terpenoids. Most substituents stabilize the product radical and carbonyl function and reduce the barrier height relative to the non-substituted template molecule ethoxy ($CH_3–CH_2O^\bullet$). The only exceptions occur where the α- or β-carbons are involved in a double bond (in addition to the breaking bond) or where C_β is part of a 3-membered ring. This observation simplifies the degradation mechanisms for some poly-unsaturated hydrocarbons. Systems, where the product radicals form a conjugated π-system with the newly formed C=O double bond, have a different A-factor by a factor of ~2.

The quantum chemical data on the alkoxy radicals are also the basis for an isomerisation SAR. Due to the ring structure of the H-shift TS, the number of rotamers to consider is significantly less than for the alkoxy radicals themselves, such that the calculations on the decomposition SAR also represent the bulk of the data for the isomerisation SAR.

3.2.2 *Site-specific SARs for OH and NO_3 addition on (poly)alkenes*

A paper was recently published (*Peeters et al*., 2007) presenting the site-specific OH-addition on (poly)unsaturated hydrocarbons. The predictions were re-examined against the latest kinetic data recommendation available in the literature. Statistical analyses of preliminary higher-order SAR expressions, e.g. accounting for H-abstraction contributions, were used to identify the source of the residual errors, including dependencies on ring strain, competing reaction channels, presence of conjugated π-systems, and other functionalities. In addition, the hypotheses underlying the SAR were also compared against the mechanistic knowledge from high-level theoretical work in the literature, which is currently viewed as a double-TS approach (*Greenwald et al.,* 2005). Finally, direct experimental measurements of the site-specificity of the OH-addition were extensively described.

Summarizing, the site-specific rate of addition can be predicted based on the stability type of the radical formed after addition (see table below); the total rate of addition $k_{tot} = \sum k_i$ is equal to the sum of addition rates over all addition sites. Isolated double bonds lead to primary, secondary or tertiary product radicals, whereas conjugated double bonds potentially lead to allyl-resonance stabilized product radicals where the rate coefficient $k_{first/second}$ depends primarily on the first radical site next to the addition site, with an additional effect of the substitution around the second resonance radical site.

Table 5: SAR parameters (10^{-11} cm^3 s^{-1}, 298K) for addition of OH on a (poly)alkene

k_{prim}	= 0.43	k_{sec}	= 3.0	k_{tert}	= 5.5
		$k_{sec/prim}$	= 3.0	$k_{tert/prim}$	= 5.7
		$k_{sec/sec}$	= 3.7	$k_{tert/sec}$	= 8.3
		$k_{sec/tert}$	= 5.0	$k_{tert/tert}$	= 9.9

Software is being developed for automated application of this SAR through a web interface. This implementation will also be used in the development of the H-abstraction SAR to combine addition- and abstraction contributions in a total rate coefficient.

The SAR predictions for total NO_3 radical addition rates on alkenes are in very good agreement with literature data, except for conjugated alkadienes, which are underestimated by about a factor of 3 (linear alkadienes) or 10 (cyclic alkadienes). The reasons for this discrepancy are unclear, but two mechanistic models are currently under investigation using quantum chemical characterizations of the TS. Furthermore, analysis of the residual errors of the SAR predictions versus the experimental data indicates that H-abstraction might be contributing for a small percentage. Literature is being searched for experimental product studies that might provide support for this view.

3.2.4 *H-abstraction from substituted hydrocarbons by OH-radicals*

The H-abstraction SAR is the first project in our research group based predominantly on the "Science project" software framework to manage the large amounts of data generated in the quantum chemical data, and the subsequent verification and incorporation in the SAR. This framework has been partly developed in the frame of IBOOT, and has reached a sufficient level of maturity to be used in a well-controlled production environment, though SAR-specific modules are still under development. The quantum chemical calculations for the SAR have started, and the results are available on a prototype website (http://arrhenius.chem.kuleuven.be/~luc/sar_habstr), currently listing over 20 alkanes and about 50 distinct H-abstraction products, with hundreds of conformers, using B3LYP/6-31G(d,p), B3LYP/cc-pVTZ and MPW1B95/6-31+G(d,p) levels of theory. Some simple SAR models are also generated, but currently these mainly serve as a test for the software rather than a production-quality predictive SARs. The MCM Review panel has provided us with an updated extensive list of available experimental data on VOC+OH-reaction for use in this Task.

3.3 Development of terpene oxidation mechanisms

3.3.1: *OH-initiated oxidation of α- and β-pinene* (KULeuven)

In a recent publication (*Vereecken et al.*, 2007), we upgraded our earlier explicit mechanism on the OH-initiated oxidation of α-pinene (*Peeters et al.*, 2001), based on very high-level quantum chemical and theoretical-kinetic calculations and theoretical-kinetic calculations, showing the importance of H-shift reactions and ring closure reactions versus reactions with NO for certain peroxy-radical intermediates. The newly incorporated chemistry explains the formation of some heavy poly-

oxygenated products observed in mass spectrometric studies available in the literature, but for which no formation channels were confirmed yet. The predicted formation of hydroperoxides and (hydroxy-)(di-)carbonyl compounds influences the predicted SOA formation in the oxidation of α-pinene (see also Sect. 3.4.3). These new developments represent a significant contribution to the current knowledge of SOA precursors, and similar reactions must be considered in the oxidation of all (sesqui)terpenes to ensure correct models.

The OH-initiated degradation mechanism for β-pinene was investigated using a combination of SAR-predictions, quantum chemical calculations, multi-conformer TST, and chemical activation estimates. The results are incorporated in a generic kinetic model, accounting for variations in the concentrations of NO_x, HO_2 and different classes of RO_2 radicals, ranging from the pristine environment up to oxidative laboratory reaction conditions. The simultaneous development of the mechanism and kinetic model ensures that all relevant reaction pathways are investigated without devoting too much effort to pathways of lesser importance.

The initial reaction of OH radicals with β-pinene can occur on nine different sites, of which addition onto the exocyclic double bonded carbon is by far the dominant channel. The chemistry following this addition is strongly influenced by the non-traditional chemistry, e.g. (per)oxy radical ring closure (*Vereecken et al.*, 2007), found earlier to also influence the α-pinene degradation. This results in a complex, highly branched mechanism with a large number of competing H-shift and decomposition pathways. We also investigated the product distribution of the most important H-abstraction channel, leading initially to an allyl-resonance stabilized alkyl radical. These two entrance channels investigated account for over 90% of the product formation.

The product distribution predictions of the current generic model indicate good results for e.g. acetone and nopinone yields. Unfortunately, no detailed experimental data is available on the plethora of high-mass poly-substituted oxygenates predicted as the main products. Finalization of this research is expected in late 2008.

3.3.2: *O_3-initiated oxidation of mono- and sesquiterpenes* (KULeuven)

The work on SOA formation in **α-pinene** oxidation described in Sect. 3.3.3 and 3.4.3 incorporates a mechanism for α-pinene ozonolysis which still lacks (theoretically) confirmed routes for the formation of the SOA precursors pinic acid (as well as peroxy-pinic acid) and hydroxy-pinonic acid. Note that we have shown that the currently accepted gas-phase formation routes for pinic acid are not viable, as crucial steps are completely outrun by competing channels (*Peeters et al*., 2001; *Capouet et al.,* 2007). Novel pathways that hold promise for efficient formation of these acids are still under theoretical investigation, such as non-traditional peroxy radical reactions, akin to those already shown to be important in the OH-initiated oxidation of α-pinene, and/or as demonstrated by us to explain byproduct formation in the liquid-phase autoxidation of cyclohexane (*Hermans et al*., 2007).

In order to quantitatively predict all important *first-generation* products of α-pinene ozonolysis, the mechanism of this major process was newly investigated theoretically in great detail, using the B3LYP/6-311++G(3df,3pd) // B3LYP/6-311G(d,p) level of theory, complemented by TST and RRKM-Master Equation (ME) statistical-kinetics approaches. A total of ca. 100 minima and 200 transition states have been located and characterized. The computed barriers for the initial O_3-addition to form the *trans*- and *cis*-ozonides, of 1 and 2 kcal/mol, are in line with the experimental Arrhenius activation energy of 1-1.5 kcal/mol; also, the multi-conformer TST-calculated total rate coefficient, $k(T) = 5.6 \times 10^{-24} \times T^{2.9}$ for T = 200-500 K, is in agreement with the experimental data (*Khamaganov and Hites*, 2001; *Atkinson et al*., 1982). An important new finding is that the chemically activated *trans*- and *cis*-ozonides – which interconvert rapidly over an energy barrier of only 7 kcal/mol – result in *four* distinct Criegee intermediates (CI) (i.e. *syn*-CI-1, *anti*-CI-1, *syn*-CI-2 and *anti*-CI-2). Due to the high barriers (of *ca*. 37 kcal/mol) for the *syn*/*anti* conversions, their interconversion is orders of magnitude slower than the fast 1,4-H shifts or ring-closures which initiate the various hydroperoxide- and ester-channel pathways of the four CI's. These latter isomerization routes, leading to the first-generation products (including $^{\bullet}$OH radicals and pinonic acid), were investigated quantum-chemically

in much detail. RRKM-ME analyses on these complex routes, in order to predict quantitatively the product branching ratios, are still in progress.

Work is also in progress on **β-pinene** ozonolysis. The first reaction step is O_3-addition on the exocyclic >C=C< bond via two transition states surmounting barrier heights of 1.9 and 2.3 kcal/mol to form two different ozonides (i.e. trans- and cis-form). Interconversion between the trans- and cis-forms takes place rapidly over a small energy barrier of 2.6 kcal/mol. These ozonides with an internal energy of ca. 48.5 kcal/mol will then undergo four distinct ring-opening pathways leading to HCHO + CI-1 / CI-2 or CH_2OO + nopinone, facing barrier heights of ca. 13.0 and 18.0 kcal/mol, respectively. As a consequence, the product HCHO is expected to dominate over nopinone, in accordance with the experimental observation. A fraction of the highly chemically activated CI-1 and CI-2 can undergo 1,4-H shifts or ring-closure to hydroperoxide or dioxirane. The subsequent reactions to various secondary products such as OH radical and CO_2 are also being investigated. The relative energies of some key stationary points were refined using the highly correlated level of theory CBS-QB3. Statistical kinetic analysis based on the CBS-QB3 potential energy surface will be done in order to predict qualitatively product distributions and overall thermal rate coefficients.

It was decided to start the theoretical research on sesquiterpene ozonolysis only in late 2007, after refinement of the methodologies to be brought to bear on pinene ozonolysis (see above). The O_3-initiated degradation of **β-caryophyllene** was investigated theoretically, using a quantum chemical characterization of the potential energy surface, in combination with statistical kinetic analysis of the initial addition reactions and subsequent (chemically activated) isomerisation and product formation. This study was recently completed (*Nguyen et al*., 2008).

The PES was characterized using B3LYP and MPW1B95 density functional methods in combination with 6-31+G(d,p), 6-311G(d,p), and 6-311++G(3df,3pd) basis sets, and supported by targeted CBS-QB3, CASSCF, and CASPT2 calculations. The (barrierless) addition channels of O_3 on the two double bonds of β-caryophyllene were examined, as well as the isomerisations to Criegee intermediates of the primary ozonides formed, and the ester and hydroperoxide channels accessible from these CI. An intersystem crossing seam for the dioxirane intermediates of the ester channel was identified, leading to a sequence of two facile decompositions yielding CO_2 as a co-product.

The thermal rate coefficients were computed using variational TST. We found that O_3-addition on β-caryophyllene occurs mainly on one side of the more reactive endocyclic double bond, whereas addition at the less reactive exocyclic double bond plays a minor role with a yield of <5%, in agreement with the experimental evidence obtained at MPI Mainz described in Sect. 3.1.3. The total rate coefficient shows a slight negative temperature dependence, and is well-described using the following Arrhenius expression:

$$k_{tot}(T) = 8.3 \times 10^{-24} \times T^{3.05} \times \exp(1028K/T)\, cm^3\, molec^{-1}\, s^{-1}$$

Finally, the first generation product branching ratios were derived from RRKM/ME calculations. At room temperature and atmospheric pressure we find 74% thermalized Criegee intermediates, while 8 % of the adducts decompose through the hydroperoxide channel yielding $^{\bullet}$OH radicals plus vinoxy-like radicals as co-products. 18% of the adducts proceed through the ester channel, yielding 8% of thermalized acids, 0.5% thermalized organic esters, and, after intersystem crossing to the triplet surface, 9.5% decomposition products comprising CO_2 and two alkyl-like radicals. These results are again consistent with the measurements. The high molecular weight oxygenates formed are expected to have a very low vapor pressure, and could contribute significantly to formation of secondary organic aerosols (SOA).

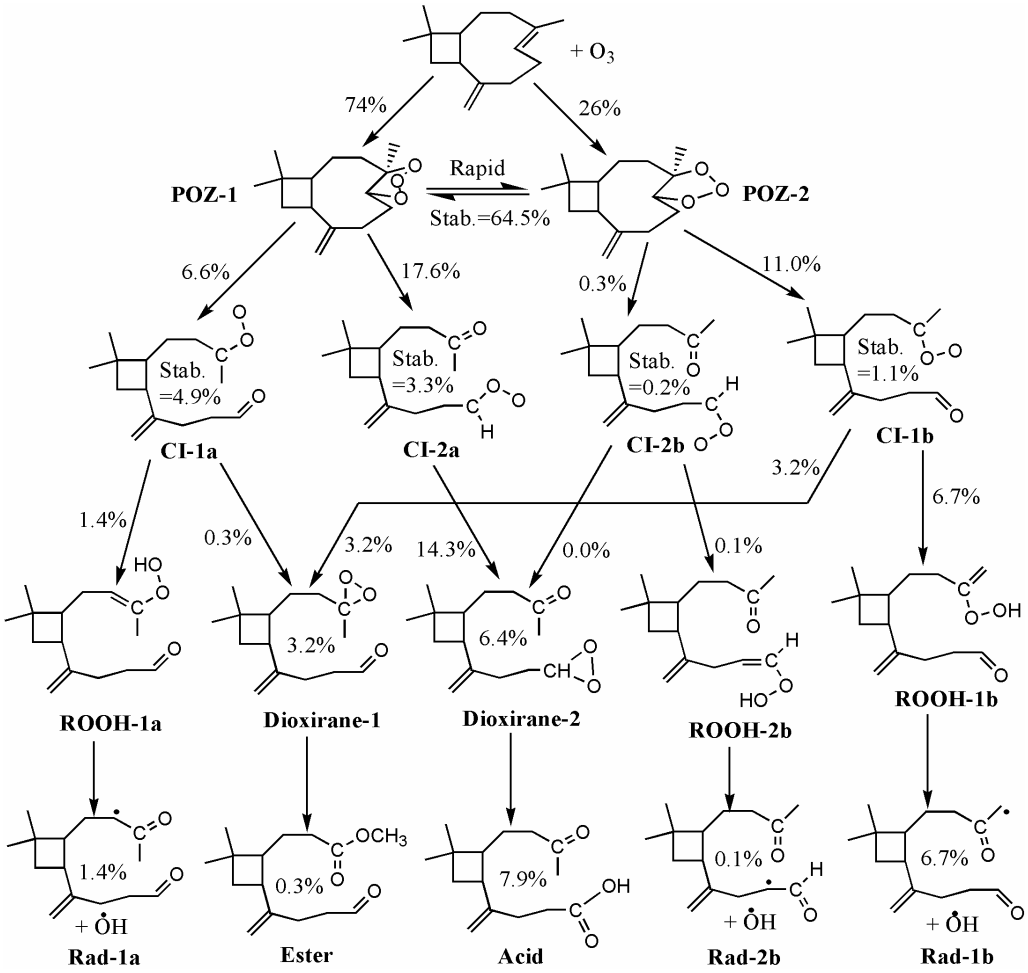

Figure 11: Schematic reaction mechanism and first generation oxidation product distribution. Branching ratios and product yields are given as absolute percentages.

A manuscript is finalized, and will be submitted for publication together with a paper describing the experimental work mentioned higher.

Preliminary work on the ozonolysis of **α-humulene** revealed that ozone addition on all three >C=C< sites proceeds without barrier, explaining the high total rate, but also implying a highly complex overall mechanism.

3.3.3: *Model simulations of terpene oxidation experiments*

The chemical box model describing the OH-oxidation of α-pinene developed in our previous work (*Capouet et al.*, 2004) has been extended to encompass a preliminary ozonolysis mechanism developed at KULeuven, as well as a simple NO_3-initiated oxidation mechanism. In addition, the new pathways proposed by *Vereecken et al.* (2007) (see Sect. 3.3.1) have been included in the mechanism.

As mentioned in Sect. 3.3.2, the ozonolysis mechanism still lacks credible pathways leading to the production of low-volatility acids such as pinic acid, which are known from experiments to be produced in significant amounts. Given their importance for aerosol growth, we implemented a crude artificial pathway leading to pinic acid, pinalic acid and hydroxypinonic acid, based on the experimental observations for the yields of these compounds (*Yu et al.*, 1999).

Note that a fully explicit terpene oxidation mechanism is out of reach with the current capabilities since the number of reactions which would be required for the explicit oxidation mechanism of a C10 alkene would be prohibitively large (*Aumont et al.*, 2005). However, the impact of the degradation of the primary products might be significant even on the time scale of a laboratory experiment. We

estimate OH-reaction rates and channels based on SARs by *Neeb* (2000), modified to account for (i) strain effects due to the 4-membered ring in compounds like pinonaldehyde, based on a theoretical study (*Vereecken and Peeters*, 2002), and (ii) recent literature data for the abstraction of H atoms adjacent to a carbonyl functionality. For the addition of OH to (poly)alkenes a new SAR by *Peeters et al.* (2007) has been implemented. Photolysis rates are estimated by treating separately the different functionalities of the molecule, except for keto-nitrates and keto-aldehydes for which experimental data are available.

High-yield compounds of the α-pinene mechanism are treated explicitly in our mechanism, whereas the degradation of minor products (with yields < 5%) is assumed to generate generic peroxy radicals, as described in more detail in *Capouet et al.* (2008). Volatility classes have been introduced, so that the products of the further reactions of these generic radicals with NO, HO_2 and other RO_2s can partition between the gas and particulate phases. The chemistry of peroxy radicals follows *Capouet et al*. (2004).

The complete α-pinene degradation mechanism has been published in a web page which allows users to explore it in a convenient way (http://www.aeronomie.be/tropo/boream/). The coupled gas phase/partitioning model, BOREAM (Biogenic compounds Oxidation and RElated Aerosol formation Model) includes about 5000 reactions and 1200 species.

A preliminary β-caryophyllene ozonolysis mechanism is under development based on similarities with α- and β-pinene, and on laboratory results reported in the literature (*Hoffmann et al*., 1997; *Jaoui et al.*, 2003) and within IBOOT (WP1) – in particular the OH yield from the ozonolysis, the initiation oxidation rates and several tentatively identified products – and on the results of the theoretical study presented in Sect. 3.3.2.

3.4 Organic aerosol modeling (IASB-BIRA)

3.4.1 *Multiphase partitioning model development*

Partitioning theory

The partitioning model follows a kinetic approach (*Kamens et al.*, 1999), with partitioning coefficients evaluated following *Pankow* (1994):

with $C_{p,i}, C_{g,i}$, the equilibrium amount of species *i* per volume of air in aerosol phase and gas phase respectively, $K_{p,i}$ the partitioning coefficient, M_0 the aerosol mass per volume of air, MW_{om} the mean molecular mass in the aerosol, *T* the temperature, p_i^0 the vapor pressure and γ_i the activity coefficient. Note that the formula of Pankow transforms to Henry's law at high water content:

$$\frac{C_{p,i}}{C_{g,i}} = \frac{RT}{MW_{om}\gamma_i p_i^0} M_0 \Rightarrow \frac{C_{p,i}}{C_{g,i}} = H_i \frac{V_w}{V_{air}} RT$$

$$H_i = \frac{\rho_w}{MW_w \gamma_i^{\infty,w} p_i^0}$$

with H_i the Henry's law constant, MW_w, ρ_w the molar mass and the mass density of water, and $\gamma_i^{\infty,w}$ the infinite dilution activity coefficient of species *i* in water.

Activity coefficients

Since the aerosol is a complex mixture, the interactions between the molecules are not the same as in a pure liquid, and the activity coefficient differs from unity. As opposed to the vapor pressure, it depends on the concentration of all other species. We adopted the popular UNIFAC method (UNIversal Functional group Activity Coefficient, *Fredenslund et al.*, 1975) which approximates the liquid phase as a mixture of functional groups. The activity coefficient is decomposed into a combinatorial part γ_i^C and a residual part γ_i^R:

γ_i^C takes the difference in size of the molecules into account

$$\ln \gamma_i^C = \ln \frac{r_i}{\overline{r}} - \left(\frac{r_i}{\overline{r}} - 1 \right) + 5 \left[q_i \ln \left(\frac{q_i}{\overline{q}} \frac{\overline{r}}{r_i} \right) - r_i \left(\frac{q_i}{\overline{q}} \frac{\overline{r}}{r_i} - 1 \right) \right]$$

with r_i, q_i measures of the Van der Waals volume and surface of molecule *i*, and $\overline{r}, \overline{q}$ the mean values over all molecules. This term is relatively unimportant, except for the small molecule H_2O.

γ_i^R takes the difference of interaction between molecules into account and is given by:

$$\ln \gamma_i^R = \sum_k \nu_k^i \left(\ln Z_k - \ln Z_k^i \right)$$

$$\ln Z_k = Q_k \left[1 - \sum_m \frac{\Theta_m \tau_{km}}{\sum_o \Theta_o \tau_{om}} - \ln \left(\sum_m \Theta_m \tau_{mk} \right) \right]$$

with ν_k the stoechiometric coefficient, Z_k, Z_k^i the activity coefficient of the functional group *k* in the mixture and in pure liquid respectively, Q_k, Θ_k the surface and surface fraction of functional group *k*.

τ_{km} is an interaction parameter describing interactions between different functional groups *k,m* and is fitted to experimental data.

Interaction parameters for several functional groups of atmospheric relevance, such as nitrates or hydroperoxides, are either not known or have not been published. Therefore, we utilized the on-line SPARC calculator (http://ibmlc2.chem.uga.edu/sparc/, *Hilal et al.*, 2004) to generate activity coefficients to which we fitted the unknown interaction parameters. In SPARC, interactions between molecules are expressed in terms of molecular descriptors (molar volume, polarizability, dipole moment), which in turn are calculated from molecular structure.

Having obtained these parameters, UNIFAC has been successfully implemented in our model. At the moment, three different parameterizations are included (*Hansen et al.*, 1991; *Magnussen et al.*, 1981; *Raatikainen and Laaksonen*, 2005), but more can be added in the future.

Simulations without water uptake: impact of activity coefficients

Figure 12 compares the calculated mass yields in the ideal and non-ideal cases, when water uptake is not considered. Different symbols are for different smog chamber experiments and different colors are for different UNIFAC parameterizations.

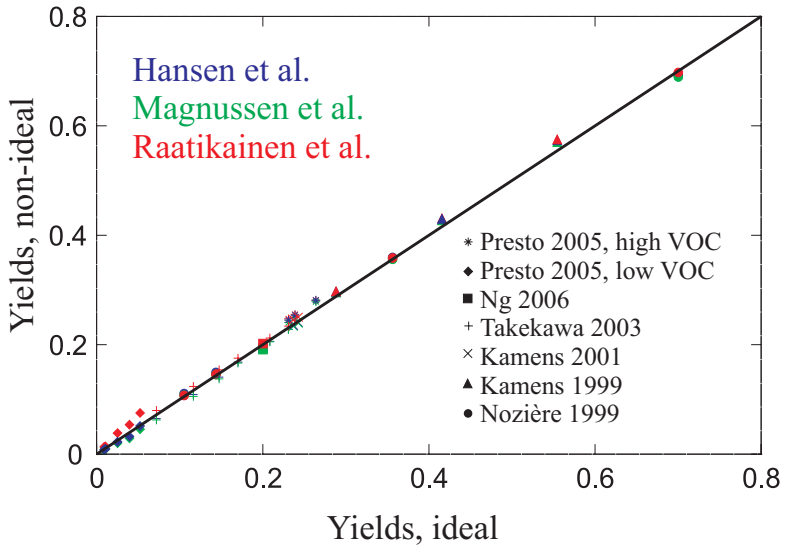

Figure 12. Mass yields, taking non-ideality into account, versus mass yields where non-ideality is not included. Water uptake is not allowed.

Non-ideality has clearly a negligible impact on the yields. It has, however, some influence on the concentrations of individual compounds. The average relative deviation of concentrations for non-ideal compared to ideal calculations defined as

is small in most cases (5-14%). In the low VOC experiments of *Presto et al.* (2005), which are closer to ambient conditions, the relative deviation is significant (11-42%).

Effect of water uptake

The effects of water condensation are multiple. The direct increase in aerosol mass due to water uptake leads to an indirect increase due to increased condensation of organic compounds. Furthermore, the activity coefficients are altered. In order to distinguish between these factors, we

calculated the effect of water uptake in both the ideal case (Figure 13, black curves) and in the non-ideal case (colored curves in Figure 13).

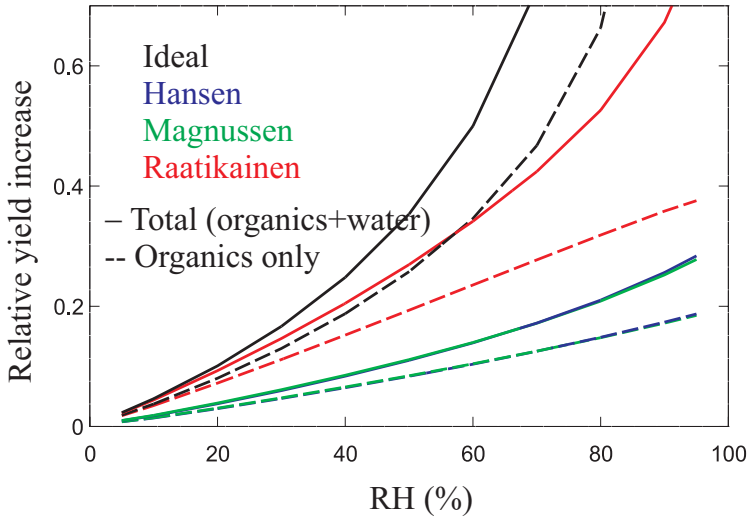

Figure 13. Relative mass yield increase due to water uptake in the ideal case (black) and in the non-ideal case, using different UNIFAC parameterizations. The dashed curves represent the contribution of organic compounds.

At moderate relative humidity (RH), the increase is mostly due to an increase in organic matter. This is due to the low molecular mass of water. Measured in molar fraction, water is important and this leads to an increased uptake of organic matter.

Non-ideality decreases the mass yield due to repulsion between water and the organic molecules. This effect depends on the precise UNIFAC parameterization. At high RH, the assumption of ideality leads to gross errors (Figure 14). Taking non-ideality - or in the limit of high RH: Henry's law- is hence necessary in these circumstances.

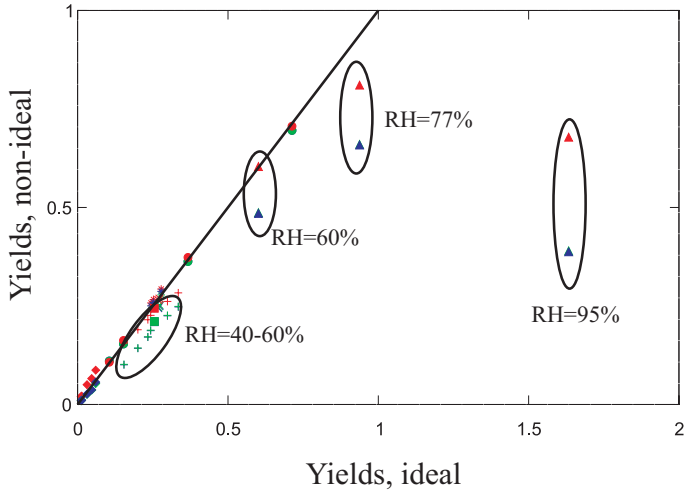

Figure 14. Same as Figure 12, with water uptake.

In conclusion, we have implemented an algorithm to calculate activity coefficients in our mechanism. At high RH, this amounts to calculating Henry's law constants for solubility. When water is not present, the impact of non-ideality is generally small but is more important for lower concentrations of α-pinene.

3.4.3 Oligomerization reactions

Recent work indicates that the oligomerization of α-pinene products can result in the formation of large, very condensable molecules. We investigated the possible impact of two such processes.

Peroxyhemiacetals from aldehydes and hydroperoxides in the liquid phase

This reversible reaction has been considered by *Tobias and Ziemann* (2000) to explain formation of peroxides in the aerosol and was investigated by *Antonovskii and Terent'ev* (1967):

$$ROOH + R'CHO \leftrightarrows ROOC(OH)R'H$$

Forward and backward rate constants are based on these experiments, although the nature of the solvent and the precise structure of the reactants could influence these rates significantly.

$$k_{fwd} = 42500.\exp(-4000/T)\left[M^{-1}s^{-1}\right]$$
$$k_{back} = 2600.\exp(-5000/T)\left[s^{-1}\right]$$

Gas phase reactions of stabilized Criegee radicals with organic compounds

Although the reaction of stabilized Criegee intermediates (SCI) with water vapor is thought to be dominant, their reactions with organic compounds can be significant at low relative humidity. Based on reaction rate measurements by *Tobias and Ziemann* (2001), we include the reactions of the SCIs from α-pinene with several acids (pinic, hydroxypinonic, pinalic, pinonic) and with pinonaldehyde, since these compounds are produced in significant yields and are strongly reactive towards the SCIs. The reaction with 2-butanol is also significant in experiments where this alcohol is used as OH-scavenger. The figure below shows an example involving pinic acid. The resulting product is a 19-carbon compound bearing many functional groups, and as a result is very condensable.

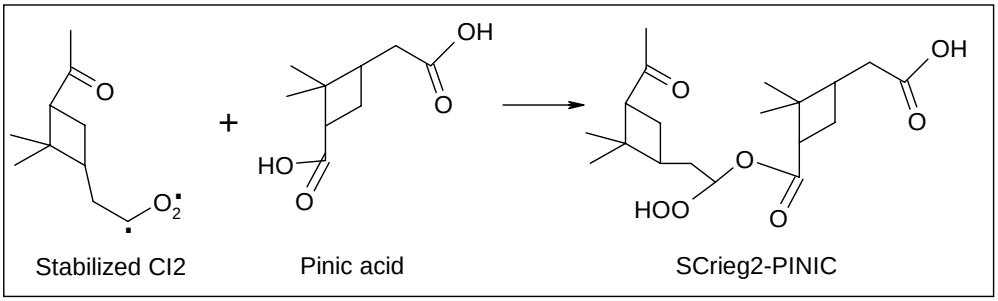

Figure 15: Reaction of a stabilized Criegee with pinic acid.

3.4.4 *Validation of aerosol model by simulation of laboratory experiments*

Photooxidation experiments

About 30 laboratory experiments of α-pinene photooxidation have been modelled, taking their specific conditions into account (actinic flux, initial concentrations, temperature, sampling time). Table 6 shows typical experimental conditions. OH and O_3 are the dominant α-pinene oxidants in *Nozière et al. (*1999*)* and *Presto et al.* (2005), respectively.

Table 6: Typical conditions of the simulated laboratory experiments. ΔHC is the reacted α-pinene, T temperature, $J(NO_2)$ the photolysis rate of NO_2. The 4th column indicates the estimated relative contribution of each oxidant to the sink of α-pinene.

	ΔHC (ppb)	ΔHC/NOx	Oxidants (%) OH : O_3 : NO_3	T (K)	$J(NO_2)$ (10^{-4} s^{-1})
Nozière et al., 1999	900	0.3	100 : 0 : 0	298	3.5 (lamp)
Kamens et al., 2001	980	2.3	42 : 44 : 14	304	35 (sun)
Hoffmann et al., 1997	95	0.8	45 : 33 : 22	315	83 (sun)
Takekawa et al., 2003	93	1.8	53 : 42 : 5	283	40 (lamp)
Ng et al., 2006	108	1.1	62 : 22 : 16	293	10 (lamp)
Presto et al., 2005	11	0.5	6 : 82 : 12	295	161 (lamp)

Figure 16 compares modelled and measured SOA yields for these experiments. The model generally reproduces the measured yields to within a factor of 2, a remarkable result considering the uncertainties on the vapour pressures and the use of an ozonolysis mechanism which lacks realistic formation pathways for the low-volatility compounds pinic acid and hydroxy pinonic acid. Objective theoretical grounds are still missing for their formation mechanisms. Differences in the vapor pressure estimations partly explain the larger SOA yields and the better agreement with the data in our model results, compared to previous modelling studies (*Jenkin*, 2004; *Chen and Griffin*, 2005). Another explanation is the more explicit treatment adopted in our mechanism for the chemistry of primary products, which generates a large variety of secondary products with different volatilities.

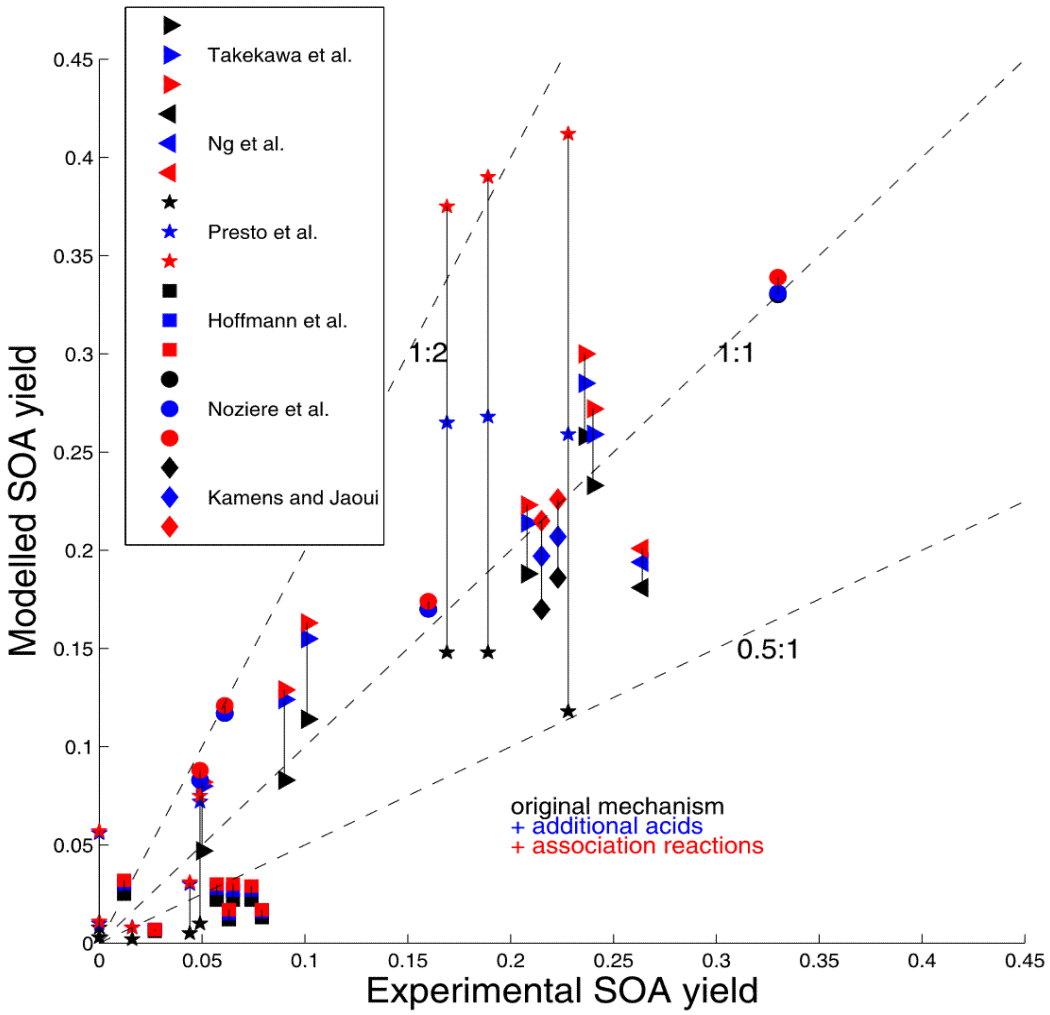

Figure 16. Modelled vs. measured aerosol yields in α-pinene photooxidation experiments. Results shown were obtained with the standard model (black) and with modified versions including additional pathways leading to low-volatility acids (in blue) and including also peroxyhemiacetal formation in the aerosol (in red).

Multifunctional compounds are dominant in the modelled SOA. Hydroperoxides make up a large fraction of SOA in low NOx conditions. The newly incorporated hydroperoxide compounds formed in the OH-initiated oxidation mechanism contribute significantly to SOA in the *Nozière et al.* (1999) experiments conducted in presence of NOx. The lower vapour pressures of hydroperoxides compared to organic nitrates explain the increase in modelled SOA yields with decreasing NOx, a result confirmed by the laboratory measurements of *Presto et al.* (2005). The contribution of generic compounds to the modelled SOA is significant, but not dominant in any case. This conclusion would not hold at later times (e.g. after several days) when most primary products would have had enough time to be oxidized. The addition of pathways leading to pinic and hydroypinonic acid in the model is seen to increase yields for experiments where ozonolysis is dominant (e.g. *Presto et al.*, 2005). Peroxyhemiacetal formation does not influence the yields significantly, except in a few cases of *Presto et al*. (2005), when aerosol yields were already high.

The model calculates that the ozonolysis produces about twice as much aerosol as the oxidation by OH in similar conditions, and the NO_3-initiated oxidation is negligible, in agreement with *Griffin et al.* (1999). A more extensive discussion of the dependence of the SOA yields on photochemical conditions and temperature is provided in *Capouet et al.* (2008).

Dark ozonolysis experiments

In Figure 17, model predictions are compared with experimental yields from a large number of dark ozonolysis experiments. Generally the model is again capable of predicting the SOA yield to within a factor 2, although there are large overestimations (for *Presto et al*., 2005 and *Iinuma et al.*) and serious underestimations (*Hoffmann et al*., 1997).

Decreasing relative humidity from 5% to 0.1% improves the agreement in the case of *Hoffmann et al.* (1997). This is due to the increased formation of oligomers from the reaction of stabilized Criegee Intermediates with organic acids, illustrating the possible importance of these reactions at low RH.

Figure 17 : Modelled versus experimental SOA yields in dark α-pinene ozonolysis experiments.

Figure 18 presents simulation results for the experiments of *Pathak et al.* (2007). Although most yields are predicted to within a factor 2, the model strongly overestimates their temperature dependence, with significant overestimations at lower temperatures (0°C-20°C) and serious underestimations at higher temperatures (30°C-40°C). The most striking underestimations are found for the experiments at 40°C, where the standard model predicts hardly any aerosol formation (0.007%) contrasting with experimental yield of the order of 9%. Clearly, the observations suggest that the yields are not very temperature sensitive, a feature not reproduced by the model. As proposed by *Pathak et al*. (2007) the production of very condensable species, which are always predominantly in the aerosol phase in the temperature interval 0°C-40°C, could explain the observations, although their production pathways remain so far unknown. The model/data bias at high temperature is reduced when stabilized Criegee radicals are allowed to react with carboxylic acids, forming oligomers. These reactions increase the simulated yield at 40°C to 0.4% at RH 1%, still more than a factor 20 too low.

Figure 18: Observed vs. simulated SOA yields for the experiments of *Pathak et al*. (2007). Triangles and circles denote model results obtained without and with oligomer formation from the stabilized Criegee Intermediates, respectively.

3.4.5 *Results for sesquiterpene oxidation experiments*

The vapour pressures of sesquiterpene oxidation products have been determined based on previous work (*Capouet and Müller*, 2006). The performance of the method is found to be lower against measurements for C10-18 compounds (*Yaws*, 1994), compared to C≤10 species, due to limitations of the method for larger compounds, and/or to the larger errors associated with the measurements of low vapour pressures. Further work will be needed to refine these estimates.

Figure 18 shows the aerosol mass formed in function of the reacted β-caryophyllene in the experiments by *Ng et al*. (2006). The agreement is good, considering the very preliminary nature of the oxidation mechanism. *Ng et al*. (2006) have observed that aerosol production continues after complete conversion of the precursor. This feature is not well reproduced by the model, probably because of oversimplification in the chemistry of the highly reactive primary products. Note that the aerosol is mainly formed of unsaturated compounds. The model calculates that the reaction of ozone with particulate-phase compounds has a significant impact on the time scale of the experiments (3 hours).

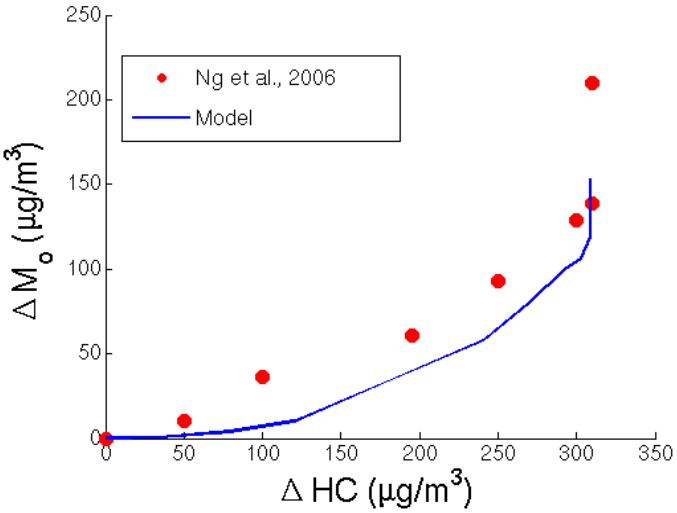

Figure 18: Secondary aerosol mass as function of the reacted β-caryophyllene.

3.5 Impact of oxygenates on the upper troposphere (KULeuven)

3.5.1: *Pressure- and temperature-dependence of reactions of oxygenates with OH*

The reactions of oxygenates with OH are characterized by the formation of H-bonded pre-reactive complexes (PRC), affecting the energy of the abstraction transition states (TS); in certain cases this even lowers the abstraction TS to below the energy of the free reactants. Using formal kinetic rate theories supplemented by multi-conformer TST calculations and RRKM-ME analyses, we showed that two regimes exist depending on the energy of the abstraction transition states relative to the initial reactants. For TS well above the free reactants, a positive T-dependence is expected, with no significant pressure dependence. Only at very low temperatures some curvature of the Arrhenius plot can occur due to tunneling through the barrier; a typical example is the reaction of acetone with OH. For TS well below the free reactants, the rate is predicted to show a pronounced dependence on pressure, because collisional energy loss of the PRC alters the competition between redissociation of the PRC and its product-forming reaction in favor of the latter. Further, a negative temperature dependence is predicted, affected by the energy dependence of the mentioned competition, the negative T-dependence of the initial, barrierless H-bond formation, and to a lesser extent tunneling. Typical examples include reactions of aldehydes or hydroxy-acetone with OH (*Peeters and Vereecken*, 2006; a full paper is in preparation). Recently we showed that an intermediate regime can exist, provided that the barrier height is within a narrow region close to the energy of the free reactants, leading to a near-T-independence over fairly large T ranges. Experimental work by Crowley et al. (MPI-Mainz), in a joint study with us, found glycolaldehyde to exhibit this extraordinary behaviour between at least 240K and 360K (*Karunanandan et al.*, 2007).

These first-principle results are fully compatible with all the available experimental literature data on the OH-initiated oxidation of partially oxygenated hydrocarbons, and represent the culmination of our theoretical work performed in previous years in the UTOPIHAN project and our collaboration with MPI-Mainz (Dr. J. Crowley).

In a continued experimental investigation of the $CH_3C(O)OH$ + OH reaction − begun under the PODO II program − we have now measured the branching fraction for the carboxyl-H-abstraction over a temperature range from 300 to 500 K, using the discharge-flow technique combined with molecular beam sampling mass spectrometry, finding this fraction to rapidly decrease from about 65% at 300 K to only some 10% at 500 K. Together with our recent experimental total rate coefficient data over the 300 - 800 K range (*Khamaganov et al.*, 2006), this confirms the gradual transition from a low-T, acidic-H-abstraction mechanism through an H-bonded PRC – showing a negative T-dependence, to (direct) methyl-H abstraction at high T – featuring a pronounced positive T-dependence. New PLP-LIF measurements of the rate coefficients of both the $CH_3C(O)OH$ and $CD_3C(O)OD$ reactions with OH, over the 295 - 800 K range, corroborate these views, showing, among others, the marked effect of

the ≈1 kcal mol^{-1} higher barrier for the D-abstraction (primary kinetic isotope effect), which brings the TS more clearly above the reactants level (see above). A second paper is in preparation.

3.5.2: *Reactions of carbonyl-bearing compounds with HO_2-radicals*

As a follow-up of our earlier work on the importance of the HO_2-initiated oxidation of formaldehyde and acetone at the low temperatures of the tropopause (*Hermans et al*., 2004 and 2005), theoretical studies have been conducted on reactions of the HO_2 radical with major (di-)carbonyl oxidation products of isoprene and terpenes. The rationale is that at these low temperatures the initial α-hydroxy-alkylperoxy adduct is stable enough to undergo subsequent, effective chemical degradation reactions with NO and HO_2. Present theoretical investigations on glyoxal and methylglyoxal have shown that such HO_2-initiated oxidation mechanisms can indeed constitute effective sinks for both these dicarbonyls near the tropopause. One key quantity for such schemes is the energy of the α-hydroxy-alkylperoxy adduct relative to carbonyl + HO_2 reactants; the *ab initio* computed value for methylglyoxal is consistent with earlier laboratory observations at room temperature (*Staffelbach et al.,* 1995). For glyoxal, we identified also a unimolecular pathway of the OCH-CH(OH)OO adduct to OH + CO + HC(O)OH; this route could play some role in laboratory experiments on glyoxal involving HO_2. A paper is to be submitted.

Directly in this context, we have also theoretically investigated the subsequent reactions of α-hydroxy-alkylperoxy adducts with HO_2. The aim was first to rationalize the recent new findings (*Jenkin et al*., 2007) that the $HOCH_2OO$ + HO_2 reaction also generates both the $HOCH_2O$ and OH radicals, besides the corresponding hydroperoxide and the acid + H_2O. We have characterized the various reaction channels involved, occurring on the triplet and singlet PES surfaces, both proceeding through H-bonded pre-reactive complexes (PRC). Our theoretical study rationalizes all observed products and their branching ratios, and reproduces the experimental absolute magnitude and T-dependence of the rate coefficient (*Burrows et al*., 1989). We predict rate coefficients at 210 K on both the singlet and triplet PES that are capture limited (i.e. formation of the PRC controls the rate), of order 5 x 10^{-10} cm^3 s^{-1}. These very high values will even enhance the efficiency of the carbonyl removal initiated by HO_2 near the tropopause, in particular at high HO_2 levels. A paper on $HOCH_2OO$ + HO_2 is to be submitted. Studies of the HO_2 reactions of the α-hydroxy-alkylperoxy adducts from glyoxal and methylglyoxal + HO_2 are still in progress.

3.7.1 *Website for Structure-Activity-Relationships*

A web site discussing the H-abstraction SAR is currently under development at http://arrhenius.chem.kuleuven.be/~luc/sar_habstr/header.html.

Bibliography

Antonovskii, V. L., and V. A. Terent'ev, *Zh. Org. Khim.*, *3*, 1011–1013, 1967

Aschmann, S. A., J. Arey and R. Atkinson, *Atmos. Environ.*, 36, 4347-4355, 2002.

Atkinson, R., A. M. Winer and J. N. Jr. Pitts, *Atmos. Environ. 16*, 1017, 1982.

Aumont, B., S. Szopa, and S. Madronich, *Atmos. Chem. Phys*., 5, 2497-2517, 2005.

Bernard, F., R. Winterhalter, A. Sadezky, G. Eyglunent, V. Daële, G. K. Moortgat and A. Mellouki, EGU, Vienna, Poster Presentation, 2008.

Berndt, T., O. Böge and F. Stratmann, *Atmos. Environ.*, 37, 3933-3945, 2003.

Bonn, B., G. Schuster and G. K. Moortgat, *J. Phys. Chem. A.*, 106, 2869-2881, 2002.

Burrows, J.P., G.K. Moortgat, G.S. Tyndall, R.A. Cox, M.E. Jenkin, G.D. Hayman and B. Veyret, *J. Phys. Chem*., 93, 2375, 1989.

Capouet, M., J. Peeters, B. Nozière, and J.-F. Müller, *Atmos. Chem. Phys*., 6, 1455-1467, 2004.

Capouet, M. and J.-F. Müller, *Atmos. Chem. Phys*., 6, 1455-1467, 2006.

Capouet, M., J.-F. Müller, K. Ceulemans, S. Compernolle, L. Vereecken and J. Peeters, *J. Geophys. Res*., 113, D02308, doi:10.1029/2007JD008995, 2008.

Chen, J. and R.J. Griffin, *Atmos. Environ*., 39, 7731-7744, 2005.

Chew, A.A. and R. Atkinson, *J. Geophys. Res.*, 101, 28649-28653, 1996.

Cocker, D. R., S. L. Clegg, R. C. Flagan and J. H. Seinfeld, *Atmospheric Environment*, 35, 6049-6072, 2001.

Donahue, N. H., K. E. H. Hartz, B. Chuong, A. A. Presto, C. O. Stanier, T. Rosenhorn, A. Robinson and S. N. Pandis, *Faraday Discuss*, 130, 295-310, 2005.

Fredenslund, A., R. L. Jones and J. M. Prausnitz, *AIChE J.*, 21, 1086-1099, 1975.

Griffin, R.J., R. C. Flagan and J. H. Seinfeld , *J. Geophys. Res*., 104, 3555-3567, 1999.

Hansen, H. K., P. Rasmussen, A. Fredenslund, M. Schiller and J. Gmehling, *Ind. Eng. Chem. Res.*, 30, 2352-2355, 1991.

Herrmann, F., Master Thesis, Johannes-Gutenberg-Universität, Mainz, December 2006.

Hermans, I., T.L. Nguyen, P.J. Jacobs and J. Peeters, *J. Am. Chem. Soc*., 126, 9908-9909, 2004.

Hermans, I., J.-F. Müller, T.L. Nguyen, P.A. Jacobs and J. Peeters, *J. Phys. Chem. A*, 109, 4303-4311, 2005.

Hermans, I., P. A. Jacobs and J. Peeters, *Chem. Eur. J*., 13, 754-761, 2007.

Hilal, S. H., S. W. Karickhoff and L.A. Carreira, *QSAR Comb. Sci.* 23, 709-720, 2004.

Hoffmann,T., J. R. Odum, F. Bowman, D. Collins, D. Klockow, R. C. Flagan and J. H. Seinfeld, *J. Atmos. Chem*., 26, 189-222, 1997.

Iinuma, Y., O. Böge, Y. Miao, B. Sierau, T. Gnauk, H. Herrmann, 130, 279-294, 2005

Jaoui, M., S. Leungsakul and R. M. Kamens, J. Atmos. Chem., 45, 261-287, 2003.

Jenkin, M.E., *Atmos. Chem. Phys*., 4, 1741-1757, 2004.

Jenkin, M.E., M.D. Hurley and T.J. Wallington, *Phys. Chem. Chem. Phys*, 9, 3149, 2007.

Johnson, D. and G. Marston, *Chem. Soc. Rev.*, 37, 699-716, 2008.

Kamens, R. and M. Jang, C.-J. Chien and K. Leach, *Environ. Sci. Technol*., 33, 1430-1438, 1999.

Kamens, R. and M. Jaoui, *Environ. Sci. Technol*., 35, 1394-1405, 2001.

Kanawati, B., S. Joniec, R. Winterhalter and G. K. Moortgat, *Int. J. Mass Spectrom.*, 266, 97-113, 2007.

Kanawati, B., S. Joniec, R. Winterhalter and G. K. Moortgat, *submitted to Rapid Commun. Mass Spectrom.*, 2008a.

Kanawati, B., F. Herrmann, S. Joniec, R. Winterhalter and G. K. Moortgat, *Rapid Commun. Mass Spectrom.*, 22, 185-186, 2008b.

Karunanandan, R., D. Hölscher, T.J. Dillon, A. Horowitz, J.N. Crowley, L.Vereecken and J. Peeters, *J. Phys. Chem. A*, 111, 897-908, 2007.

Khamaganov, V.G., and R. A. Hites, *J. Phys. Chem. A, 105*, 815, 2001.

Khamaganov, V.G., V. Xuan Bui, S.A. Carl and J. Peeters, *J. Phys. Chem. A*, 110, 12852-12859, 2006.

Koch, S., R. Winterhalter, E. Uherek, A. Kolloff, P. Neeb and G. K. Moortgat, *Atmos. Environ.*, 35, 4525-4526, 2000.

Lee, A., A. H. Goldstein, M. D. Keywood, S. Gao, V. Varutbangkul, R. Bahreini, N. L. Ng, R. C. Flagan and J. H. Seinfeld, *J. Geoph. Res.,* 111, D07302, 2006.

Lindinger, W., A. Hansel and A. Jordan A., *Chem. Soc. Rev.*, 27, 347-354, 1998.

Magnussen, T., P. Rasmussen, A. Fredenslund, *Ind. Eng. Chem. Proc. Des. Dev.,* 20, 331-339, 1981.

Neeb, P., F. Sauer, O. Horie and G.K. Moortgat, *J. Atmos. Chem*., 35, 295-315, 2000.

Ng, N.L., J. H. Kroll, M. D. Keywood, R. Bahreini, V. Varutbangkul, R. C. Flagan, J. H. Seinfeld, A. Lee, and A. H. Goldstein, *Environ. Sci. Technol*., 40, 2283-2297, 2006.

Nguyen, T.L., G. Moortgat, R. Winterhalter, B. Kanawati, J. Peeters and L. Vereecken, in preparation, 2008

Nozière, B., I. Barnes and K. H. Becker, *J. Geophys. Res*., 104, 23645-23656, 1999.

Pankow, J. F., *Atmos. Environ*., 28, 185-188, 1994.

Pathak, R. K., C. O. Stanier, N. M. Donahue and S. N. Pandis, *J. Geophys. Res*., 112, D03201, 2007.

Paulson, S. E, A. Sen, P. Liu, J. Fenske and M. Fox, *Geophys. Res. Lett.*, 24, 3193-3196, 1997.

Peeters, J., L. Vereecken and G. Fantechi, *Phys. Chem. Chem. Phys.*, 3, 5489-5504, 2001.

Peeters, J. and L. Vereecken, 19th International Symposium on Gas Kinetics, Orleans (France), 2006.

Peeters, J., W. Boullart, V. Pultau, S. Vandenberk and L. Vereecken, *J. Phys. Chem. A*, 111, 1618-1631, 2007.

Presto, A.A., K. E. H. Hartz and N. M. Donahue , *Environ. Sci. Technol*., 39, 7046-7054, 2005.

Raatikainen, T. and A. Laaksonen, *Atmos. Chem. Phys.,* 5, 2475-2495, 2005.

Rickard, A. R., D. Johnson, C. D. McGill and G. Marston, *J. Phys. Chem. A.*, 103, 7656-7664, 1999.

Römpp, A., R. Winterhalter and G. K. Moortgat, *Atmos. Environ.*, 40, 6848-6862, 2006.

Staffelbach, T.A., J.J. Orlando, G.S. Tyndall and J.G. Calvert, *J. Geophys. Res.*, 14, 189, 1995.

Sadezky, A., P. Chaimbault, A. Mellouki, A., Römpp, R. Winterhalter, G. Le Bras and G. K. Moortgat, *Atmos. Chem. Phys.*, 6, 5009-5024, 2006.

Sadezky, A., R. Winterhalter, B. Kanawati, A. Mellouki, G. Le Bras, A. Römpp, B. Sprengler, P. Chaimbault and G. K. Moortgat, *Atmos. Chem. Phys.* 8, 2667-2699, 2008.

Shilling, J. E., Q. Chen, S. M. King, T. Rosenoern, J. H. Kroll, D. R. Worsnop, K. A. McKinney and S. T. Martin, *Atmos. Phys. Chem.*, 26, 1193-1205, 2008.

Shu, Y. and R. Atkinson, *Int. J. Chem. Kin.*, 26, 1193-1205, 1994.

Siese, M., K. H. Becker, K. J. Brockmann, H. Geiger, A. Hofzumahaus, F. Holland, D. Mihelcic and K. Wirtz , *Env. Sci. Techn.*, 35, 4660-4667, 2001.

Stenby, C., U. Pöschl, P. Von Hessberg, M. Bilde, O. J. Nielsen and G. K. Moortgat, *Atmos. Chem. Phys. Discuss*., 7, 2091-2132, 2007.

Takekawa, H., H. Minoura and S. Yamazaki, *Atmos. Environ*., 37, 3413-3424, 2003.

Tobias, H. J. and P. J. Ziemann, *Environ. Sci. Technol*. , 34, 2105-2115, 2000.

Tobias, H. J. and P. J. Ziemann, *J. of Phys. Chem. A*., 105, 6129-6135, 2001.

Vereecken, L. and J. Peeters, *Phys. Chem. Chem. Phys*., 4, 467-472, 2002.

Vereecken, L., J.-F. Müller and J. Peeters, *Chem. Phys. Phys. Chem*, 9, 5241-5248 , 2007.

Winterhalter, R., P. Neeb, D. Grossmann, A. Kolloff, O. Horie and G. Moortgat, *J. Atmos. Chem.*, 35, 165-197, 2000.

Yaws, C., Handbook of Vapor Pressure, Gulf Publ. Company, Houston, 1994.

Yu, J. , D. R. Cocker, R. J. Griffin, R. C. Flagan and J. H. Seinfeld, *J. Atmos. Chem.*, 34, 207-258, 1999.

4. PERSPECTIVES FOR PHASE 2

4.1 Laboratory studies of mono-and sesquiterpenes ozonolysis (Mainz)

***Task 1.1**: Products and reaction mechanism of the reaction of ozone with the sesquiterpenes α-humulene and β-caryophyllene*

The studies will focus on the reaction of ozone with the α-humulene, since in the first phase mainly β-caryophyllene has been investigated. For the analysis of gas-phase products (e.g. CO, CO_2, HCOOH and HCHO) on-line FTIR spectroscopy will be applied. Particulate products will be sampled on filters and analyzed by liquid chromatography coupled to mass spectrometry (LC-MS-MS-TOF). The reaction of Criegee-Intermediates formed by decomposition of the primary ozonide, with H_2O is a NO_x-independent source of hydroperoxides (ROOH) and will be investigated at various relative humidities. Furthermore, experiments with other Criegee-intermediate scavengers like HCOOH and HCHO will also be performed in order to further clarify the reaction mechanism. Since OH-radicals are formed in course of the ozonolysis, different OH-radical scavengers (cyclohexane, butanol) will be added and their influence on the product formation investigated.

***Task 1.2**: Determination of aerosol yields from sesquiterpene-ozonolysis*

In the first phase the aerosol yields of β-caryophyllene have been determined and in the second phase the studies will focus on α-humulene. Aerosol particle size distributions will be measured by a Scanning Mobility Particle Sizer (SMPS), which enables to determine the aerosol yields. The influence of the different reaction conditions (as defined in Task 1.1) on the aerosol yields will be determined at T = 298 K in order to draw conclusions about different SOA formation pathways. It is known that the aerosol yield increases with decreasing temperature and therefore experiments in a temperature controlled flow reactor (275 K < T < 305 K) will be performed to determine the temperature dependence of the aerosol yields.

***Task 1.3**: Identification and quantification of organic peroxides from mono- and sesquiterpene-ozonolysis*

The applicability of Atmospheric Pressure Photoionization (APPI) will be explored as another mass spectrometric method for detection of higher organic peroxides, since the detection with ESI and APCI ionization methods was not possible.

***Task 1.4**: Formation of oligomers and polymers from mono- and sesquiterpene-ozonolysis*

The formation of oligomers and polymers from the ozonolysis of mono- and sesquiterpenes will be investigated. The potentially formed oligomers or polymers will be analysed by LC-MS-MS-TOF. Specially designed extraction procedures will be developed, since the so far proposed polymers might easily be hydrolyzed upon extraction of the filter samples with water.

***Task 1.5**: Determination of CCN activity of mono- and sesquiterpene-ozonolysis products*

An important factor in cloud formation is the hygroscopicity of the aerosol particles, which is commonly determined by a Tandem-DMA method and from the hygroscopic growth factor conclusions about the cloud condensation nuclei (CCN) activity of aerosol particles are drawn. We will measure the CCN-activity of the aerosol particles formed from mono- and sesquiterpene-ozonolysis directly with a CCN-counter in collaboration with the Biogeochemistry Department of the Max Planck Institute for Chemistry.

4.2 Development of predictive tools for mechanism development (KULeuven)

Our research is guided by (i) high-level quantum chemical calculations using Density Functional Theory, Complete Active Space, Coupled Cluster, and Gaussian-method extrapolations, complemented by (ii) advanced theoretical kinetics calculations to obtain the temperature- and pressure dependent rate coefficients and product distributions, using the best suited methodologies. Systematic studies along these lines, in combination with experimental data, will allow the development of Structure-Activity Relationships (SARs) for a number of key atmospheric reaction types:

Task 2.1: *SARs for alkoxy radical decomposition and isomerization*

A SAR for the decomposition and isomerization of (multi-)substituted alkoxy radicals formed during the degradation of organic compounds, in particular terpenes, and of oxygenated organics. The importance of oxygenates commands that our previously developed SAR [*Peeters et al*. 2004] (i) be extended to other substituents, including those from carboxylic acids, ethers, esters, peroxides; and (ii) that it incorporate the effects of (vinoxy-type) resonance stabilization and of intramolecular hydrogen bonding.

Task 2.2: *Site-specific SARs for NO_3 addition reactions on unsaturated hydrocarbons*

Due to the bi-pronged attack of NO_3 on the double bond, the addition depends not only on the product radical site, but also on the addition site. A SAR for NO_3-addition is being developed.

Task 2.3: SAR for cycloadddition of O_3 to (poly-)unsaturated hydrocarbon:

Ozone is the dominant oxidant of many terpenes. Combined with detailed quantum computations, the abundant available data on the rate of cycloaddition of O_3 will provide a basis for a general SAR.

Task 2.4: *SAR for H-abstraction in substituted hydrocarbons by OH-radicals*

H-abstraction by OH is a dominant initiation step for saturated hydrocarbons. For each stabilization mode of the radical formed, a well-defined quantitative relationship (correlation >0.97) is found between abstraction rate and the calculated bond strength. Quantification of these relations will result in a powerful predictive SAR for these reactions.

4.3 Development of terpene oxidation mechanisms

Task 3.1 *OH-initiated oxidation of pinenes*

During the first phase, the degradation mechanism for α-pinene has been improved by incorporating novel pathways discovered in earlier work (*Vereecken and Peeters*, 2004). This enhanced mechanism has been tested in modeling work, showing the importance of this new chemistry. Current results on the OH-initiated β-pinene degradation show that these reactions are also the likely cause of the severe discrepancy between experimental data and model predictions; by extension, the chemistry of other poly-unsaturated compounds, including mono- and sesquiterpenes, could be affected by these reactions. A complete mechanism for the β-pinene+OH degradation is under development.

Task 3.2 *O_3-initiated oxidation of mono- and sesquiterpenes*

We intend to develop explicit mechanisms for the O_3-initiated degradation of α-pinene, α-humulene, and β-caryophyllene, using theoretical methodologies as in WP 2. In addition, we will investigate the possible pathways leading to compounds detected in field studies, including those conducted by the BIOSOL project.

The mechanisms constructed in Tasks 3.1 and 3.2 can serve as templates for other mono- and sesquiterpenes, as well as for other unsaturated VOCs The identification of formation channels for large poly-functional oxygenates are crucial to improve the predictions on the formation of secondary

organic aerosols. Our study will focus primarily on the formation of (di-) carboxylic acids and multi-hydroxy-substituted aldehydes and ketones.

Task 3.3 *Model simulations of terpene oxidation experiments*
The focus during Phase 1 has been on the simulation of α-pinene oxidation experiments. This work will be continued. The parameterized treatment developed in our previous work for the degradation of the primary products will be refined and extended, given its great importance in atmospheric conditions. We will also incorporate new mechanistic information obtained by our Partner at KULeuven, when available. The impact of gas-phase oligomerization reactions (e.g. reactions of Criegee Intermediates with organics, association reaction of peroxy radicals) will be investigated. Next, we will implement a detailed ozonolysis mechanism for the sesquiterpene β-caryophyllene. Its oxidation by OH and NO_3 radicals can be neglected due to their high reactivity towards ozone. This mechanism will be tested by the simulations of laboratory results obtained from smog chamber studies, such as *Jaoui et al.* (2003). We will check the ability of the model to reproduce the observed product yields and (when available) the time-dependent concentrations of reactants and products under various conditions. The ozone formation potential of β-caryophyllene degradation will be also tested using laboratory measurements, including the chamber data of the SAPRC at University of California (*Carter et al.*, 2000).

4.4 Organic aerosol modeling (Brussels)

Given the inability of current models to explain the formation of oligomers and the presence of many semi-volatile products (e.g. carbonyls) in the aerosol phase, it appears necessary to account for water uptake, heterogeneous and particle phase-phase reactions. Important examples of such processes include the reactions of gaseous oxidants with particulate organics, the particle-phase association reactions of carbonyls and hydroperoxides, and the hydration of carbonyls. These processes are often promoted by liquid water and acidity. For this reason, we are currently extending the BOREAM model in order to account for water uptake, hydration, phase-splitting and other processes. The new model will be tested by comparison with other methods and will be adopted to estimate the formation of SOA from the oxidation of (sesqui)terpenes.

Task 4.1 *Thermodynamic properties of oxidation products*
The vapor pressures of sesquiterpene products will be determined by extending the group contribution method developed previously (*Capouet and Muller*, 2005). We have shown in Phase 1 that activity coefficients of water and organics can be derived from the UNIFAC prediction method. Henry's law constants of (sesqui)terpene oxidation products will be derived from the activity coefficients and vapor pressures, and tested against the available experimental data by *Sander* (1999).

Task 4.2 *Multiphase (gaseous/aqueous/organic) partitioning model development*
During Phase 1 of the project, a purely organic aerosol model has been developed, based on the absorptive theory of *Pankow* (1994) and on the product distribution of the oxidation mechanism developed at KUleuven. In Phase 2, the liquid water content of the aerosol will be determined, based on existing methods reviewed and tested during Phase 1. When water and SOA form a single phase, the liquid water content is determined simply from its vapor pressure and activity coefficient. However, multiple liquid phases can arise when inorganic salts and/or hydrophobic primary organic are present, affecting the uptake of organics and water. Several models taking into account ion-water and ion-organic interactions exist (e.g. *Raatikainen* 2005, *Erdakos* 2006) and the most appropriate one will be implemented. The modeled water uptake will be verified against experimental data on hygroscopic properties of organic aerosols. The model will be coupled to an existing thermodynamic model for inorganic aerosols, like the SCAPE2 model (*Kim et al.*, 1993a,b).

Task 4.3 *Validation of aerosol model by simulation of laboratory experiments*
The comparisons of our model results with dark ozonolysis experiments presented in this report will be completed and presented in a publication. The impact of activity coefficients and water uptake will be evaluated. In the framework of the European project EUROCHAMP, we will simulate a large number of

laboratory experiments of α-pinene degradation, and our results will be compared with both the data and the other participating models. We will also simulate the plant growth chamber experiments of the BIOSOL project (Task 1.1.2). SOA formation from β-caryophyllene ozonolysis will be investigated and the model results will be confronted to the laboratory results obtained under WP 1 as well as in previous studies. This study will allow us to perform a comparative analysis of the SOA formation potential of the different terpenes considered.

Task 4.4 *Exploratory study of heterogeneous reactions in organic aerosols*
Given the complex and speculative nature of the many aerosol-phase processes proposed to explain the observed organic aerosol composition, we will focus first on the well-documented case of glyoxal, a compound often found in atmospheric aerosols, and for which aerosol-phase reactions have been proposed (*Warneck*, 2003; *Liggio et al.*, 2005). The particulate-phase reactions of larger carbonyls (e.g. pinonaldehyde) with hydroperoxides have been already considered during Phase 1. The heterogeneous reactions and their resulting low-volatility products will be included in the model described above, and their influence on aerosol yields and composition will be estimated.

4.5 Impact of oxygenates on the upper troposphere (KULeuven)

The degradation pathways of certain oxygenated hydrocarbons, including their temperature and pressure dependence has been extensively investigated during the first phase of the project and in earlier work. This includes work on acetic acid, acetaldehyde, propionaldehyde, hydroxyacetone, glycolaldehyde, (methyl)glyoxal, etc., in some cases putting some new reaction channels in evidence (Hermans et al., 2005), or disproving reported channels (Vandenberk et al., 2002). Intramolecular H-bonding often results in highly unusual temperature dependences and unexpected reaction channels, making a generalized description of this reaction class difficult. In order to quantify and formulate general trends, we propose to continue in-depth theoretical study of the fate of small oxygenates in the higher troposphere and lower stratosphere, by theoretically studying the temperature and pressure dependent reaction kinetics of such compounds with OH and/or HO2. DF-MBMS and PLP-LIF apparatus is available to help verify the findings experimentally.

4.6 Global modeling (Brussels)

Task 6.1 *Development of reduced mechanism for the oxidation of mono- and sesquiterpenes by OH and* O_3

A reduced oxidation mechanism for the terpenes will be implemented, based on the semi-explicit mechanism developed in WP 3. This reduced mechanism will be tested against the detailed mechanism using the box model in low- as well as high-NOx conditions.

Task 6.2 *Development of SOA parameterization for use in a global model*

SOA formation from terpenes will be parameterized based on the reduced mechanism and a simplified representation of the (aqueous and organic) aerosol phase will be implemented based on the aerosol model developed in WP 4. Both hydrophilic and hydrophobic Primary organic aerosols (POA) will be also included. In a later stage, the distributions of inorganic aerosols calculated by the coupled IMAGES-SCAPE2 model (*Rodriguez and Dabdub*, 2004) will be used, and partitioning of SOA on these aerosols will be tentatively taken into account. Alternatively, the IMAGES-SCAPE2 model could be extended and coupled to the SOA module, so that the effect of inorganic ions on the aqueous aerosol phase (liquid water content and acidity) could be explicitly taken into account.

Task 6.3 *Validation of global model for OC and NMVOC against field studies, including BIOSOL measurements*

The calculations of the global model IMAGES for OC and NMVOC will be validated against field studies, in particular the OC measurements of the BIOSOL project (Task 1.2). The BIOSOL estimates

for the contribution of BVOC SOA and biomass burning to OC (Task 3 of BIOSOL) will be also compared with the model estimates.

Task 6.4 *Determination of the role of terpenes on the global budget of oxidants and on the formation of organic aerosols*

The global impact of BVOC emissions on the budget of oxidants (O_3 and OH) will be determined, as well as a possible range for global SOA production, based on sensitivity studies on the role of uncertain parameters (e.g. sesquiterpenes emissions, chemistry of primary products, vapor pressures of polyfunctional compounds, activity coefficients) and poorly represented processes (e.g. oligomer formation, as outlined in Task 4.4). The impact of novel reaction kinetics for small oxygenates (WP 5) will be also quantified.

5. PUBLICATIONS OF THE TEAMS

5.1 In peer review journals

M.T. Nguyen, **T.L. Nguyen**, V.T. Ngan, H.M.T. Nguyen, Heats of formation of the criegee formaldehyde oxide and dioxirane, Chem. Phys. Lett., 448, 183-188, 2007.

R. Karunanandan, D. Hölscher, T.J. Dillon, A. Horowitz, J.N. Crowley, **L. Vereecken, J. Peeters,** Reaction of HO with Glycolaldehyde, $HOCH_2CHO$: Rate Coefficients (240 - 362 K) and Mechanism, J. Phys. Chem. A, 111, 897-908, 2007.

J. Peeters, W. Boullart, V. Pultau, S. Vandenberk**, L. Vereecken,** Structure-Activity Relationship for the Addition of OH to (poly)Alkenes : Site-specific and Total Rate Constants, J. Phys. Chem. A, 111, 1618-1631, 2007.

L. Vereecken, J.-F. Müller, J. Peeters, Low-volatility poly-oxygenates in the OH-initiated atmospheric oxidation of α-pinene: Impact of non-traditional peroxy radical chemistry, Phys. Chem. Chem. Phys., doi:10.1039/b708023a, 2007.

S.A. Carl, L. Vereecken, J. Peeters, Kinetic parameters for gas-phase reactions: Experimental and theoretical challenges, Phys. Chem. Chem. Phys., doi:10.1039/b705505f, 2007.

T.J. Dillon, A. Horowitz, D. Hölscher, J.N. Crowley, **L. Vereecken, J. Peeters,** Reaction of HO with Hydroxyacetone ($HOCH_2C(O)CH_3$): Rate Coefficients (233 - 363 K) and Mechanism, Phys. Chem. Chem. Phys., 8, 236-246, 2006.

V.G. Khamaganov, V. Xuan Bui, **S.A. Carl, J. Peeters,** Absolute Rate Coefficient of the OH + $CH_3C(O)OH$ Reaction at T = 287-802 K. The Two Faces of Pre-reactive H-Bonding, J. Phys. Chem. A, 110, 12852-12859, 2006.

A. Römpp, **R. Winterhalter** and **G. K. Moortgat**, Oxodicarboxylic acids in atmospheric aerosol particle, Atmos. Environ., 40, 6848-6862, 2006.

C. Stenby, U. Pöschl, P. Von Hessberg, M. Bilde, O. J. Nielsen and **G. K. Moortgat**, Temperature and humidity dependence of secondary aerosol yield from the ozonolysis of β-pinene, Atmos. Chem. Phys. Discuss., 7, 2091-2132, 2007.

B. Kanawati, S. Joniec, **R. Winterhalter** and **G. K. Moortgat,** Mass spectrometric characterisation of small oxocarboxylic acids and gas phase ion fragmentation mechanisms studied by Electrospray Triple Quadrupole-MS/MS-TOF system and DFT Theory, Int. J. Mass Spectrom., 266, 97-113, 2007.

B. Kanawati, F. Herrmann, S. Joniec, **R. Winterhalter** and **G. K. Moortgat**, Mass spectrometric characterisation of β-caryophyllene ozonolysis products in the aerosol studied by an electrospray triple quadrupole and time-of-flight analyzer hybrid system and density functional theory, *Rapid Comm. Mass Spectrom.,* 22, 185-186, 2008.

A. Sadezky, P. Chaimbault, A. Mellouki, **A. Römpp**, **R. Winterhalter**, G. Le Bras and **G. K. Moortgat,** Formation of secondary organic aerosol and oligomers from the ozonolysis of enol ethers, Atmos. Chem. Phys., 6, 5009-5024, 2006.

A. Sadezky, **R. Winterhalter, B. Kanawati**, A. Mellouki, G. Le Bras, **A. Römpp**, B. Sprengler, P. Chaimbault and **G. K. Moortgat**, Oligomer formation during gas-phase ozonolysis of small alkenes and enol ethers: new evidence for the central role of the Criegee Intermediate as oligomer chain unit, Atmos. Chem. Phys., 8, 2667-2699, 2008.

M. Capouet, J.-F. Müller, A group contribution method for estimating the vapour pressures of alpha-pinene oxidation products, Atmos. Chem. Phys., 6, 1455-1467, 2006.

M. Capouet, J.-F. Müller, K. Ceulemans, S. Compernolle, L. Vereecken, J. Peeters, Modeling Aerosol Formation in Alpha-pinene Photooxidation Experiments, J. Geophys. Res., 113, D02308, doi:10.1029/2007JD008995, 2008

submitted :

T. L. Nguyen, **L. Vereecken, J. Peeters,** HO_2-iniated oxidation of glyoxal, methylglyoxal and glycolaldehyde in atmospheric and laboratory conditions : a theoretical study, J. Phys. Chem. A, submitted, 2007.

T.L. Nguyen, M.T. Nguyen, **J. Peeters,** Reaction of hydroxyl radical with methyl-hydroperoxide (OH + CH_3OOH): A theoretical study, J. Phys. Chem. A, submitted (2007)

Kanawati, B., S. Joniec, **R. Winterhalter** and **G. K. Moortgat,** Mass spectrometric characterisation of 4-oxocarboxylic acid and gas phase fragmentation mechanisms studied by Electrospray Triple Quadrupole-MS/MS-TOF system and DFT theory, J. Mass Spectrom., submitted, 2008.

in preparation :

Nguyen, T.L., G. Moortgat, R. Winterhalter, B. Kanawati, J. Peeters and L. Vereecken, The gasphase ozonolysis of β-caryophyllene ($C_{15}H_{24}$): A theoretical study, in preparation, 2008

Herrmann, F., B. Kanawati, R. Winterhalter, G. K. Moortgat, L. Vereecken, T. L. Nguyen and J. Peeters, The ozonolysis of β-Caryophyllene: kinetics and mechanistic investigations of new products in the secondary organic aerosols, *in preparation (2008).*

Related work:

J.-F. Müller, T. Stavrakou, S. Wallens, A. Guenther, M. Potosnak, J. Rinne, B. Munger, A. Goldstein, Global isoprene emissions estimated using MEGAN and a detailed canopy environment model, Atmos. Chem. Phys., 8, 1329-1341, 2008.

I. Hermans, P.A. Jacobs**, J. Peeters,** To the Core of Autocatalysis in Cyclohexane Autoxidation, Chem. Eur. J., 16, 4229-4240, 2007 (VIP paper and cover)

I. Hermans, J. Peeters, P.A. Jacobs, Autoxidation of ethylbenzene: The mechanism elucidated, J. Org. Chem., 72, 3057-3064, 2007.

I. Hermans, P.A. Jacobs**, J. Peeters,** The formation of byproducts in the autoxidation of cyclohexane, Chem. Eur. J., 13, 754-761, 2007.

5.2 Others

M. Capouet, Modeling the oxidation of alpha-pinene and the related aerosol formation in laboratory and atmospheric conditions, PhD Thesis, Université Libre de Bruxelles, 2006.

F. Herrmann, Produkte und Reaktionsmechanismen des Sesquiterpeneozonolyse, Diplom Thesis (Master) at Johannes-Gutenberg University Mainz, December 2006.